Report 51: Valuing lives, education and the economy in an epidemic: Societal benefit of SARS-CoV-2 booster vaccinations in Indonesia

Rob Johnson[1], Bimandra Djaafara[1,2], David Haw[1], Patrick Doohan[1], Giovanni Forchini[1,3], Matteo Pianella[1], Neil Ferguson[1], Peter C Smith[4,5], and Katharina D Hauck[1*]

[1]MRC Centre for Global Infectious Disease Analysis & WHO Collaborating Centre for Infectious Disease Modelling, Jameel Institute for Disease and Emergency Analytics, Imperial College London, United Kingdom
[2]Eijkman-Oxford Clinical Research Unit, Jakarta, Indonesia
[3]USBE, Umeå Universitet, SE-901 87, Umeå, Sweden
[4]Department of Economics and Public Policy, Imperial College Business School, United Kingdom
[5]Centre for Health Economics, University of York, United Kingdom
[*]Correspondence: k.hauck@imperial.ac.uk

SUGGESTED CITATION

Summary

Countries face competing priorities in responding to the SARS-CoV-2 pandemic. The key trade-off is between deaths and pandemic mitigation that reduces SARS-CoV-2 transmission via mandated closures of non-essential economic activity and schools. Vaccinations are one of the key interventions to address this trade-off. They not only reduce deaths, but also the need for policy makers to implement socially damaging and economically costly pandemic mitigation measures. There is little comprehensive quantitative evidence on the societal benefit of vaccinations. Here, we project the socio-economic gains of vaccinations in terms of averted deaths, averted economic losses and averted educational losses with the dynamic epidemiological and economic model Daedalus, applied to Indonesia. We model a twelve-month Moderna booster vaccination campaign, beginning in September 2021, with 80% target coverage against a counterfactual of no boosters. We assume the booster campaign is delivered against a background of optimised epidemic mitigation with economic and school closures that are gradually eased, double-dose vaccinations reaching 90% of the eligible population, and epidemiological characteristics of the Delta and Omicron variants in sensitivity analyses.

We find that the total expected socio-economic gain of the booster campaign is $381 billion (95% confidence interval $260-$640) for our central scenario. It comprises of 19 million years of in-person education, $81 billion in economic activity, and 300,000 life-years (or 14,000 deaths). Depending on monetary valuations of education and life years, the expected gain ranges from $365 billion to $608 billion. The social benefit of each Moderna dose ranges from $2,000 (95% confidence interval $1,400-$3,100) to $3,300 ($2,600-$5,200). Projected gains per dose are higher for a booster vaccination campaign with 40% target coverage at $2,200 ($1,200-$3,300) to $4,200 ($3,400-$6,600).

Our findings are sensitive to the decision makers' valuations of life years and education, and to the unpredictable evolution of the virus. However, results are very similar for epidemiological parameters corresponding to the Delta and Omicron variants. Our results demonstrate that the majority of benefits of vaccination manifest in the reduced need for costly mitigation, rather than averted deaths. This calls for a comprehensive modelling of the benefits of vaccinations focusing not only on health impacts, but also on economic and social impacts.

1   Introduction

In responding to the COVID-19 pandemic, there is a trade-off between competing priorities for societies. Policy interventions designed to protect public health by limiting the face-to-face interactions that enable transmission also limit the interactions that facilitate economic activity, education and other desirable social and societal goods. Policy makers therefore have to trade off the costs of their interventions in terms of the society's overall welfare, which includes health, education, and economic welfare (Robinson et al., 2019). Vaccinations are highly effective in preventing severe COVID-19 disease and deaths, as well as limiting transmission (Meslé et al., 2021). It has been estimated that SARS-CoV-2 vaccinations have saved nearly half a million lives among those aged 60 years and over in 33 countries across the WHO Euro region in less than a year (Meslé et al., 2021). The benefits of vaccinations are not only measurable in terms of saved lives, but also in terms of reduced duration and stringency of pandemic mitigation required to control transmission. Nearly all countries are adopting pandemic mitigation measures, including closures of economic activity and education, to control the pandemic while vaccination coverage is too low to achieve control. However, we do not currently have estimates of the comprehensive societal welfare gain of SARS-CoV-2 vaccinations arising from both averted deaths and reduced need for costly pandemic mitigation via business and school closures.

Here, we estimate the societal benefits of vaccinations in terms of gross domestic product (GDP), deaths averted, and person-years of education gained under alternative vaccination scenarios and mitigation strategies in Indonesia. We specify a loss function, relying on existing monetary estimates of the value of education, economic activity, and lives (Bloom et al., 2020). We use an existing integrated economic-epidemiological model DAEDALUS (Haw et al., 2020) to project the societal benefits of a moderate and an expedited Moderna booster vaccination campaign against a no-booster counterfactual. While boosters are scaled up, we assume that the social planner adopts optimised pandemic mitigation that minimises societal costs, trading off the costs of school and business closures against deaths.

The cost of lives lost due to the pandemic has been estimated in terms of the value of a statistical life (Hammitt, 2020; Robinson et al., 2021) and as the expected loss to the economy due to deaths and illness of the workforce (Fernald et al., 2021). We consider both in our projections, using estimates of a value of a statistical life for Indonesia (Wulandari, 2020; Robinson et al., 2021). The cost of reduced economic activity due to the pandemic and its mitigation has immediate, mid- and long-term implications (International Monetary Fund, 2021*a*; Jordà et al., 2020). These have been estimated for individual countries by charting losses incurred so far and projecting forwards what the cost will be in the decades to come (Sawada and Sumulong, 2021; Cutler and Summers, 2020). We consider short- and mid-term economic costs related to the pandemic and its mitigation, relying on GDP projections of the International Monetary Fund for Indonesia (International Monetary Fund, 2021*a,b*).

The immediate costs to individuals and businesses are lost earnings and revenues. In many high-income countries (HICs), these are mitigated by relief policies such as furlough payments, tax relief or other support programs. However, in low- and middle-income countries (LMICs) with a high proportion of informal employment and constrained public budgets, the scope for relief policies is often small. This implies that households and businesses are hard hit by mitigation strategies that curtail economic exchange. The short-term economic costs of business closures have been estimated at around 25% of pre-pandemic GDP in HICs (Haw et al., 2020), to which the costs of relief policies must be added.

Because of the severe and immediate economic costs of business closures, the limited scope for relief policies, and

the high proportion of informal sector work that can effectively resist officially mandated closures, many LMICs, including Indonesia, cannot rely much on mitigation via closure of economic production. Instead, countries use long-term closure of in-person education to reduce transmission of SARS-CoV-2 (The World Bank et al., 2021). In Indonesia, schools were closed for in-person teaching for 18 months, from March 2020 to August 2021. Because the education sector contributes little to GDP (e.g. in Indonesia in 2019, the education sector contributed 3.4% to GDP among 36 sectors), but contributes much to transmission, mitigation policies that prioritise school closures are associated with lower economic losses in the short term.

However, conventional measures of the gross value added (GVA) of the education sector grossly underestimate the true value of education. The benefits of education lie in future economic gains across all sectors, through having a better educated, more skilled and more productive workforce (Hanushek and Woessmann, 2020). These gains are not captured by contemporaneous national account calculations. For example, it was estimated that education losses will contribute more than one quarter of the total pandemic losses expected to the Philippine economy over the next four decades (National Economic and Development Authority, 2021). We use estimates of the long-term benefits of education for Indonesia from the OECD to provide more realistic projections of the benefits of in-person education resulting from avoided school closures.

2   Methodology

2.1   DAEDALUS: integrated economic-epidemiological model

We use the Daedalus model (Haw et al., 2020) to fit and simulate the dynamics of the epidemic in Indonesia using publicly available data. Details of the model specific to this application, its parameterization, the data used to fit the model, and the result of the model fit, are given in Appendices A, B, and C. We compare economic configurations through their socio-economic costs across three categories (losses to lives, education, and economic output), relying on valuations from external sources for a year of life lost (YLL), and a year of education.

We model the economy as consisting of 36 sectors, following the ISIC 4 classification (UN Economic and Social Affairs, 2008). We assume that policy makers can partially close economic sectors as pandemic mitigation. We describe the resulting economic configuration as the set over all sectors i and months τ: $\{x_{i,\tau} : i \in \{1, ..., 36\}; \tau \in \{1, ..., T\}\}$ for T months, where $x_{i,\tau}$ is defined as a sector's output in month τ relative to its maximum possible value, which is the output when $x_{i,\tau} = 1$ and there is no mandated closure. Sector 33 is the education sector, and all the other sectors without education are denoted x_{-33} for ease of exposition. In Daedalus, the economic configuration forms the basis to compute the economic output over the projection period, and determines the extent of transmission between different population groups.

For the months February 2020 to August 2021, we estimate $x_{i,\tau}$ as the sector's observed output relative to its pre-pandemic output according to GVA data (see Appendix A.2 for details). For the education sector, $x_{33,\tau}$ corresponds to the fraction of students engaged in in-person teaching. To project the impact of alternative pandemic mitigation scenarios, we choose values for $x_{i,\tau}$ to reflect possible policy choices. We require $x_{i,\min} \leq x_{i,\tau} \leq 1$ to ensure essential production capacity for each sector (Table 7).

The economic configuration determines the number of individuals in workplaces via an analogous set $\{w_{i,\tau}\}$, where $w_{i,\tau}$ is defined as the proportion of the workforce present in the workplace under sector closure $x_{i,\tau}$. We estimate

the active workforce given the specified sector closure assuming a non-linear relationship between workforce and production for the non-education sectors. Specifically, the fraction of total workers required to produce a fraction $x_{i,\tau}$ of total output is $w_{i,\tau} = x_{i,\tau}^{1/\alpha}$.[1] For education, as $x_{33,\tau}$ represents school opening rather than production, we define $w_{33,\tau} = x_{33,\tau}$ so that the fraction of teachers in school is the same as the fraction of students.

The compartmental epidemiological model consists of 40 population groups: one group for each sector, and one group per age group (ages 0-4, 5-19, 20-64, and 65 plus). Each individual belongs to only one group at any one time. The 20-64 group comprises of (a) individuals who are not in the labour force, e.g. because they are home-makers, and (b) individuals in the labour force (workers) who are not currently working because their sector is closed. Workers may change group membership from their sector to the 20-64 group (and back) at the start of each month, following sector closures/openings. The fraction of each sector working at time τ is given by $w_{i,\tau}$, which defines the size of the labour force that is working. We use $\{w_{i,\tau}\}$ to determine the extent of workplace-related transmission directly by moving workers between their sector groups and the 20-64 group, and indirectly by scaling the number of contacts per person that facilitate transmission of infection, which covers the effects of working from home and commuting, as described in Haw et al. (2020). Interactions that are modified by the extent of remote learning and use of commercial spaces are similarly scaled according to how open the relevant sectors are as defined by $x_{i,\tau}$.

2.2 Determining socio-economic costs

By assigning monetary values to YLLs and to years of education, we can add health and education costs of mitigation strategies to the costs of economic closures, and undertake a comprehensive comparison of economic configurations based on socio-economic costs. A summary of the costs we take into account and those we do not is given in Table 1.

We define the total socio-economic costs, SC, of an economic configuration $\{x_{i,\tau}\}$ for the T-month duration by first specifying a general formula for the loss function. For simplicity, we assume a simple linear function where we add together terms for each of the costs:

$$SC = f_{\text{education}}(X, \text{VSY}) + f_{\text{lives}}(D, l, \text{VLY}, r) + f_{\text{GDP}}(Z_0 - Z, r). \tag{1}$$

Here, X is the number of school years lost (defined in Section 2.2.1), and VSY is the value of one school year, measured in \$; D is the number of deaths per age group due to COVID-19, l the remaining life years expected per age group, VLY is the value of one life year, measured in \$, and r is the discount rate; $Z_0 - Z$ is the lost output over the period due to reduced economic activity, measured in \$, where Z_0 would be the maximum possible in a fully open economy, and Z the output generated. The longer-term cost of the short-term economic loss is defined in the function $f_{\text{GDP}}(Z_0 - Z, r)$. The cost can exceed the loss if there is damage done to the economy beyond the temporary loss of income. Then the socio-economic cost is the sum of the costs vs. a no-pandemic counterfactual (i.e. no mandated school or economic closures, and no loss of life to COVID-19).

We here assume a simple product for the function $f_{\text{education}}$, and a nonlinear function for the cost of lost output over the period $L = f_{\text{GDP}}(Z_0 - Z, r)$ (defined in Section 2.2.5). For f_{lives}, we combine terms D, l and r into a single term Y, which is the total "discounted" years of life lost due to COVID-19 (see Section 2.2.2):

$$SC = X * \text{VSY} + Y * \text{VLY} + L. \tag{2}$$

---

[1]For this application, we use $\alpha = 0.46$; see Appendix A.2 for details and assumptions made.

Importantly, the cost includes both immediate costs, and mid- to long-term costs, all attributable to choices made about closures over a short time period. The losses are added up over all years for which the loss is expected to persist, using the same discounting rate r of 3%, which is implicit in the valuation of a school year (VSY) and applied to the other losses. As the counterfactual no-pandemic scenario has a cost of 0, Equation 2 represents the sum total socio-economic costs of the pandemic over the period in question. We now describe the computation of the socio-economic costs.

2.2.1   Valuing lost education

Education loss is quantified as the effective number of years of schooling lost. In each month τ, education is divided into a fraction of in-person teaching $(w_{33,\tau})$ and remote teaching $(1 - w_{33,\tau})$. We compute the total amount of education completed as a weighted sum of the school opening and its complement, where remote teaching contributes a fraction s of the educational value of in-person teaching. The loss then is the amount of remote teaching $(1 - w_{33,\tau})$ multiplied by the value lost in remote teaching $(1 - s)$, multiplied by the number of people of school age and the number of years under consideration (disregarding school holidays):

$$X = \frac{1}{12} \sum_{\tau} (1 - s)(1 - w_{33,\tau}) \sum_{g \in \text{school age}} N_g, \tag{3}$$

where N_g is the number of people in age group g. We consider only the second age group out of four (5 to 19 years) to be school-age students.

Remote teaching in Indonesia is thought to add a value of around one third of classroom teaching $(s = \frac{1}{3})$ considering infrastructure coverage, household access and effectiveness of teaching (Yarrow et al., 2020). This aligns with an analogous estimate for the Philippines of 37% (National Economic and Development Authority, 2021).

We consider two alternative estimates for the value one year of education adds to the economy over a person's lifetime. Both valuations express the cost of education loss as a percentage of GDP. For the first valuation, we use estimates from a study that projects the loss to GDP growth from a workforce cohort that is less skilled than that which preceded it (who completed their education in 2020) and that which will follow it (who will begin their education after schools reopen). It was assumed that growth will be impacted for the following 52 years (a cohort of 12 years with careers expected to last 40 years), and the expected costs were estimated up to the year 2100 assuming a 3% discount rate (Hanushek and Woessmann, 2020). Applying the findings of Hanushek and Woessmann (2020), we value the loss of a year of education for the current school cohort at 202% of current GDP, and obtain a value of $34,000 for a person–year of schooling in Indonesia. For the second valuation, we adapt a projection of educational losses in the Philippines (National Economic and Development Authority, 2021), for whom one year of remote teaching (at 37% the effectiveness of in-person teaching) was estimated to have cost the economy 10.7 trillion pesos, which equates to one full year lost to 89% of the country's GDP in 2019. Applied to Indonesia, the value of a year of education per student is $15,000.

We assume that there are no short-term costs related to school closures, including that the Government's spending to enable remote learning (e.g. $400 million, spent mainly on data packages (Purnamasari and Ali, 2021)) does not change with school openings. We also assume that there is no impact of school closure on the size of the available workforce. We do not correct the estimated loss of education for individuals who die, nor consider the loss of education due to sickness of teachers or students. The former means we overestimate the amount of education lost, and the latter that we underestimate it.

2.2.2   Valuing lost lives

To value lives lost, we make use of the expected remaining life years, l_g, per age group g (Global Burden of Disease Collaborative Network, 2021). The life years lost per death with discounting taken into account can be written

$$\hat{l}_g = \sum_{y=1}^{l_g} \frac{1}{(1+r)^y} \tag{4}$$

for discount rate $r > 0$. The discounted number of years lost given D_g deaths due to COVID-19 for each age group is

$$Y = \sum_g D_g \hat{l}_g, \tag{5}$$

We use this notation to define the cost as a simple product of VLY and the discounted number of years for input into Equation 2.

The value of a year of life (VLY) used by policy makers should reflect the valuation that members of the society place on reductions of their own mortality. We rely on the intrinsic rather than instrumental interpretation of the valuation of life (Cutler and Summers, 2020), and we use existing estimates of the value of a statistical life (VSL) to estimate VLY. Following Ananthapavan et al. (2021) and Robinson et al. (2021), the population VSL equals the population-weighted average VSL, where each age group has a VSL defined by the number of expected life years remaining, and where each year has the same value (VLY) with discount rate r:

$$\text{VSL} = \frac{\sum_g N_g \hat{l}_g}{\sum_g N_g} \text{VLY}. \tag{6}$$

We use two alternative existing estimates for the VSL in Indonesia. First, we use the value of $950,000 for a life of a working-age individual (Wulandari, 2020). With 38 years remaining life expectancy for this group, we get an estimate for VLY of $42,000. Second, we use an estimate of one VSL being worth 160 times GNI per capita (based on purchasing power parity, following Robinson et al. (2021)), which we evaluate to be $1,910,000, giving a VLY of $80,000. We do not take into account any health costs apart from lives lost due to COVID-19.

Finally, we define the value of lives lost as

$$f_{\text{lives}}(D, l, \text{VLY}, r) = \text{VLY} * Y. \tag{7}$$

In the results, we report the total YLLs,

$$\text{YLL} = \sum_g D_g l_g,$$

in their natural units of years, and, separately, the monetized life years lost, $f_{\text{lives}}(D, l, \text{VLY}, r)$, in $.

2.2.3   Valuing lost economic output

We measure the cost of economic closures in terms of lost gross value added (GVA): the GDP generated by an economic configuration is the maximum GVA per month (denoted z_i for each sector i) multiplied by the respective sector openings, summed over the period. The maximum possible GDP (which is with no closures for T months) is $Z_0 = T \sum_i z_i$, and we use pre-pandemic output to define the maximum possible values.

2.2.4 Short-term GDP loss

Recall that $x_{i,\tau}$ denotes how open sector i is in month τ. This in turn determines the proportion of the workforce contributing to economic production, $w_{i,\tau}$, out of the total workforce N_i. The workforce is not only reduced due to mandated closures, but also due to sickness, hospitalisation and death, leaving a smaller fraction $(\widehat{w}_{i,\tau})$ to contribute to production.[2] The output for the remaining workforce is $\widehat{x}_{i,\tau} = \widehat{w}_{i,\tau}^{\alpha}$. Then the total GVA for the period is:

$$Z = \sum_{i \neq 33} \sum_{\tau=1}^{T} z_i \widehat{x}_{i,\tau} + T z_{33} \tag{8}$$

and the GDP loss compared to the maximum is $Z_0 - Z$. All economic sectors contribute GVA according to the level they are open for production, except for the education sector which contributes its maximum possible monthly GVA, z_{33} per month. Note that the economic output lost due to absence (symptomatic infection, hospitalisation, and death) is negligible compared to other costs (Figure 3).

2.2.5 Mid-term GDP loss

It is questionable whether the economy bounces back to its pre-pandemic level of production immediately after the mandated closures end. To model the mid-term impact of the pandemic and mandated closures of non-essential businesses, we estimate hypothetical growth paths for each scenario, relying on existing estimates of economic recovery for Indonesia. Following projections by the IMF (International Monetary Fund, 2021*a*,*b*), we assume that no long-term scarring will occur as a result of the economic losses; however, there will be a period of lower than expected output until the currently projected GDP path is rejoined. We allow mid-term economic cost to accumulate over six years, by projecting the economic losses arising from a delayed return of the economy to the counterfactual or reference GDP path.

We define the reference path as the GDP, measured in \$, projected by the IMF for the years 2021 to 2026 (International Monetary Fund, 2021*b*). We denote the reference path $G_y^{\text{(ii)}}$ for $y = 2021, ..., 2026$. The scenario path, which we denote $(*)$, begins with the observed GDP for 2020 and the IMF-projected GDP for 2021 minus the short-term GDP loss: $\left\{ G_{2020}^{(*)}, G_{2021}^{(*)} \right\} = \left\{ G_{2020}^{\text{(ii)}}, G_{2021}^{\text{(ii)}} - (Z_0 - Z) \right\}$.

To project the scenario path forward in time, we estimate the scenario-specific growth path that is required for the scenario path to converge to the reference path in five years (Figure 1, left). The growth from 2020 to 2021 is less in the scenario than in the reference growth path. Therefore, for the GDP paths to converge, the scenario growth must at some point exceed the reference growth. To estimate the necessary growth, we make use of two vintages of IMF estimates: made in April 2021 and October 2021, and denoted (i) and (ii), respectively. When comparing these two estimates, it is obvious that the IMF revised growth for 2021 downwards, presumably to reflect the larger-than-expected hit to the economy. Still, the IMF projected that the original GDP path would be rejoined. We apply the same reasoning and the same mechanism to our scenarios so that they converge to the reference path (Figure 1, right).

Defining the growth rate

$$v_{y+1}^{(\cdot)} = \frac{G_{y+1}^{(\cdot)} - G_y^{(\cdot)}}{G_y^{(\cdot)}},$$

---

[2] $\widehat{w}_{i,\tau} = w_{i,\tau} - \sum_v \mathbb{E}_{d \in \tau} \left(I_{S,v,i}(d) + H_{v,i}(d) + D_{v,i}(d) \right) / N_i$ for vaccine status v, infectious and symptomatic I_S, hospitalised H, deceased D, with total population N_i for sector i. $\mathbb{E}_{d \in \tau}$ represents that we compute the average number for all days d in month τ.

which is known for the IMF projections (i) and (ii) and the first year for the scenario, we extract the growth rate for the scenario, $v_y^{(*)}$, for $y > 2021$ by solving

$$\frac{v_y^{(*)} - v_y^{(ii)}}{v_{2021}^{(*)} - v_{2021}^{(ii)}} = \frac{v_y^{(ii)} - v_y^{(i)}}{v_{2021}^{(ii)} - v_{2021}^{(i)}}. \tag{9}$$

Then the scenario GDP path will converge to GDP path (ii), in the same way that GDP path (ii) converges to GDP path (i), given the initial divergence in GDP in the year 2021.

Then we write the scenario path as

$$G_{y+1}^{(*)} = G_y^{(*)} \left(1 + v_{y+1}^{(*)}\right). \tag{10}$$

The total economic cost of closures is then given by

$$L = \sum_{j=0}^{5} \frac{G_{2021+j}^{(ii)} - G_{2021+j}^{(*)}}{(1+r)^j}. \tag{11}$$

Where the time period spans a year change, we split Z (and Z_0) into their component parts $Z^{(2021)}$ and $Z^{(2022)}$. Then $G_{2021}^{(*)} = G_{2021}^{(ii)} - \left(Z_0^{(2021)} - Z^{(2021)}\right)$, and $G_{2022}^{(*)} = \left(1 + v_{2022}^{(*)}\right) G_{2021}^{(*)} - \left(Z_0^{(2022)} - Z^{(2022)}\right)$. Then the convergence to the reference path is modelled as before, starting from the year 2022.

In summary, we project economic costs of each scenario via the deviations of the projected scenario GDP paths from the IMF reference GDP path from the year 2021 onward until 2026. This implies that we are assuming that closure decisions impact short- and mid-term economic output but not long-term growth and GDP of the Indonesian economy, in line with IMF assumptions. (Figure 1, right).

2.3   Decision problem of the social planner

We use a decision framework to decide the mitigation policies consisting of closures of businesses and schools to keep transmission under control, which provides the background to the vaccination programme. We assume that a social planner is choosing between a set of discrete options which make up the decision space, and chooses the option that minimises the socio-economic costs (see e.g. Figure 2). The decision space consists of the choice of school opening and the choice of business closures. The costs of closures are directly traded against the costs of deaths associated with each choice, so that the optimal choice is the one with the smallest total SC.

In the decision space, school opening takes values 10 (10% open), 20, …, 100% (fully open). The business closure takes values 0 (fully open), 0.5, …, 4 (maximum hypothetical closure). The business closures are defined in relation to the observed reference closure in 2021, given by observed sectoral GVA. A relative closure of 1 means that the closure is the same as the reference. The maximum observed closure for any sector over the period gave 78% of pre-pandemic GVA; therefore, at four times closure, this sector will be open at only 12%. It is questionable whether such stringent closure is feasible, but we include this as an extreme lower bound to economic output in sensitivity analyses. By scaling observed closure configurations according to observed GVA, we honour inter dependencies between the sectors in their supply chains. We do not allow closures of sectors which did not exhibit closures in the past, under any of our configurations.

As an illustration of the social planner's decision problem, we compare observed economic and health outcomes in Indonesia over the period May to August 2021 to those that would have minimised total SC in a retrospective
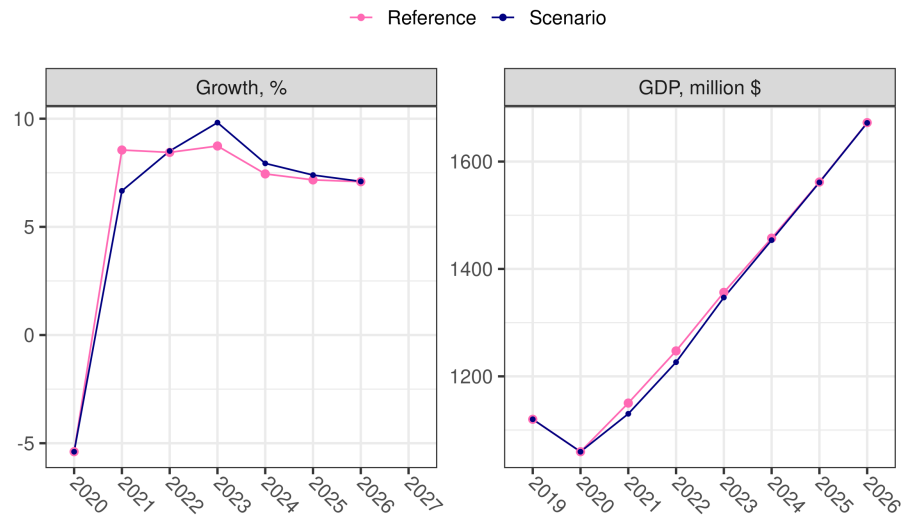
Figure 1: Projections of Indonesian's growth and GDP, 2019 to 2026. Left panel: the scenario growth rate is computed using the reference growth rate as in Equation 9. We adjust the growth rates for the Scenario following IMF projections from April and October 2021 so that in the year 2026, the reference path projected by the IMF in October 2021 has been rejoined. Right panel: Scenario GDP is projected over time using Equation 10. The cost to the economy is estimated as the difference between the GDP obtained under the scenarios and the IMF reference GDP, summed over the years 2021 to 2026, as defined in Equation 11.

analysis. We use four valuation sets for education and health, arising from all combinations of the two valuations for lost school years and life years, respectively (Table 2). We use valuation set 2 for our central scenarios, but present results for all four sets. The same business and school closures are applied to each of the four months.

2.3.1 Booster vaccination scenario analysis

By the beginning of September 2021, 2.5% of school-age individuals, 19% of working-age adults, and 29% of people over 60 had received two doses of Sinovac in Indonesia. For our simulation, we assume that Sinovac vaccine rollout continues for these age groups (the "target group") with the same administration rate as in August 2021, and is distributed between the three age groups such that after twelve months the coverages are 90% in each group. To achieve this, we stipulate that 87.5% of all school-age individuals, 71% of all working-age adults, and 61% of all people over 60 are vaccinated in the 365-day period with the same number of people within each group vaccinated each day. We assume that one booster vaccine dose can be given to someone who has been double vaccinated with Sinovac. Indonesia has already started to give Moderna boosters to healthcare workers; therefore, we assume that all boosters will be Moderna. For simplicity, we assume a constant vaccine administration rate also for the booster doses over the projection horizon. We consider three scenarios for the administration of boosters over the twelve-month period from September 2021 to the end of August 2022: None, coverage of 40% among three target age groups by the end of the period with no particular prioritization, and coverage of 80% among the target groups.

Parameters defining vaccine effects and waning in the model are summarised in Table 8. The profile of vaccine effects for the Moderna booster are defined using recent estimates for overall effects of a BNT162b2 (Pfizer) booster given after two doses of Sinovac (Jara et al., 2022), which were presented together with corresponding estimates for two doses of Sinovac. Delta was the predominant lineage circulating at the time of the study and thus we

Table 1: Summary of costs we model and costs we omit.

Cause	*Immediate costs*		*Mid- to long-term costs*	
	Modelled	Not modelled	Modelled	Not modelled
School closure		Reduced productivity of parents	Loss of earnings	Probability to drop out University closures
Student illness and deaths		Reduced productivity of parents		Loss of earnings
Business closures	Reduced GDP	Increased poverty	Delayed return to GDP path	Increased poverty
Worker illness and deaths	Reduced GDP		Delayed return to GDP path	Reduced workforce
COVID-19 deaths	Life years lost (valued)			
COVID-19 illness		Medical care		Reduced quality of life Reduced life expectancy
Strained health services[a]		Other health outcomes		Other health outcomes
Stay-at-home orders[b]		Other health outcomes		Other health outcomes

[a] Deferral of appointments and procedures for conditions other than COVID-19. Deferral can be due both to limited capacity of health services and to individuals choosing not to engage with health services in times of high prevalence.

[b] Stay-at-home orders impact on individuals' mental and physical health, and will have costs in the short term and the long term.

take these estimates as an appropriate set to estimate the impact of a Moderna booster compared to a Sinovac background. The profiles of vaccine effects for protection against four outcomes (where protection manifests in the model as multiplying the rate by one minus the vaccine effect) are $(0.93, 0.26, 0, 0)$ for the Moderna booster, and $(0.5, 0.08, 0.64, 0.22)$ for Sinovac double dose, for the outcomes of: acquisition, symptomatic infection given acquisition, hospitalisation given symptomatic infection, and death given hospitalisation, respectively.

By comparing the SC of the three booster vaccine rollout scenarios, we estimate the benefit of booster doses in terms of avoided economic and school closures and deaths in the first year following initiation of the booster scheme. We use the decision framework explained above to assume background mitigation via optimal closure configurations for the year given the rollout scenario, and compute the total SC for the whole year. By choosing the optimal closure configurations for each scenario, we are effectively comparing the best-case SCs. This allows us to compute the difference in SCs associated with the two booster vaccination strategies against the no-booster counterfactual. Here, business closure is defined relative to the closure observed in February 2021, and we use the observed configurations for the period May to August 2021 based on sectoral GVA data (as detailed in Appendix A.2, rather than a hypothetical scenario configuration from Table 3).

The social planner makes two sequential decisions on configurations: First, at the start of the projection period, the planner decides on a fixed configuration for the first four months. Second, the planner decides on a linear gradient on

Table 2: Alternative valuation sets for education and life years.

Valuation sets	Value of one person-year of education (VSY, in $)	Value of a life year (VLY, in $)
Set 1	15,000	42,000
Set 2	15,000	80,000
Set 3	34,000	42,000
Set 4	34,000	80,000

opening business activity and schools linearly as vaccination coverage increases over six months, after which it stays at the final configuration for two final months. We make the decisions in two separate steps to reduce computational burden. As decisions made considering only a short time period force the next period to begin with substantial costs, we choose the four-month configuration using an eight-month projection horizon (see Appendix D.1).

As there is uncertainty in how transmission will evolve, we simulate multiple epidemiological outcomes with randomly varying epidemiological parameters and compute the SC for each simulation. We identify the optimal decision under uncertainty as the one that minimises expected SC (Briggs et al., 2006). Here, the uncertain parameter of interest is the "transmission modifier", which is the extent to which transmission is scaled, capturing changes to transmission that are driven by factors unrelated to business or school closures (see Appendix B.1), such as individuals' behaviour, other non-pharmaceutical interventions, efficiency of contact tracing, and others. We assume that future values of the modifier are likely to resemble past values, and that it changes every month. We have inferred values from fitting the model to data for months up to August 2021 (see Appendix C). For projection months, we sample with replacement from values inferred for months from April 2020 to August 2021.

For each scenario, we report total SC, and SC related to the three outcomes of interest, for the twelve-month projection period. We also report incremental SC between all three scenarios, calculated by dividing the difference in total SC by the difference in the number of administered vaccine doses, and other key outcomes, including the chosen configuration, the number of deaths, the total amount of in-person education delivered, the total GDP, and the total number of YLLs. The comparisons against the no-booster scenario tells us the quantified social benefits of moderate (40% coverage at twelve months) and expedited (80% coverage at twelve months) booster vaccination campaigns. In Appendix D.3, we undertake a hypothetical sensitivity analysis using parameter values appropriate for the Omicron variant in order to contextualise the results for the most recent phase of the pandemic. We find that the results are very similar for parameters chosen to reflect current knowledge about the Omicron variant, compared to our main projections that assume parameters corresponding to the Delta variant. In Appendix D.4, we present the main results using a modified model with additional uncertain parameters: one that determines the protective effect of the vaccine against infection, which declines over time, and one that determines hospitalisation rate, which can rise or fall over time. These uncertainties represent hypothetical new variants. In this way, the value of particular campaigns can be assessed with these uncertainties about the future taken into account. Further, we can assess how important the uncertainties are in influencing the conclusions we draw.
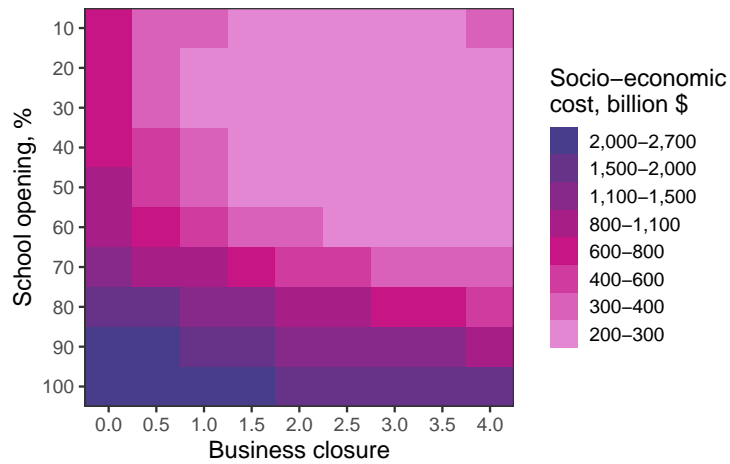
Figure 2: Socio-economic costs under alternative business and school opening configurations, May to August 2021 (Valuation set 2). For a grid of configuration options (business closures and school openings), we evaluate the socio-economic costs (SC) in order to select the configuration that minimises total SC as the optimal mitigation strategy, given valuation set 2. An unmitigated epidemic has School opening=100% and Business closure=0.0. The Observed scenario over May to August 2021 in Indonesia corresponds to schools open at 10% and businesses closed at 1.0, which is not the optimal configuration.
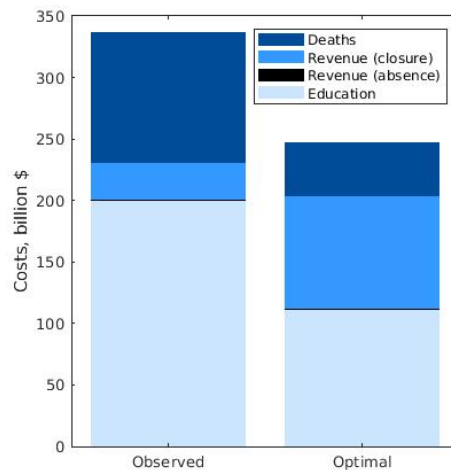

Figure 3: Socio-economic costs of observed period vs. optimal pandemic mitigation, valuation set 2, May to August 2021.

Table 3: Observed and optimal pandemic mitigation via closures of businesses and schools, four valuation sets for lost education and life years, May to August 2021.

	School opening, %	Business closure	Person-years of in-school education, millions	YLLs, millions	GDP, billion $	Economic loss, billion $	Deaths, millions
Observed	10	1.0	2.2	2.0	269	31	0.09
Valuation set 1	50	2.5	11.1	1.2	253	77	0.05
Valuation set 2	50	3.0	11.1	0.8	247	92	0.03
Valuation set 3	60	3.0	13.3	1.6	247	93	0.06
Valuation set 4	60	3.5	13.3	1.2	241	108	0.05

Note: Comparison of observed outcomes and projected outcomes for four optimal configurations (business closures and school openings) given four valuation sets for education and life years. Observed school opening was 0.1 and observed Business closure was 1 over the period, which is not the optimal configuration under any valuation set. Values for School opening and Business closure are the optimal choices for the given valuation set, i.e. they minimise socio-economic costs among all possible configurations given the valuation set. The remaining columns report outputs from the epidemiological model (YLLs, Deaths) and economic model (Person-years of in-school education, GDP) for the optimal configurations. We report the economic loss compared to the no-pandemic counterfactual, whose calculation does not depend on the valuation (Equation 11). We leave education and YLLs in natural units to allow comparison across the four valuation sets that place different values on education and YLLs.

3   Results

3.1   Illustration of decision framework and results

We present first a comparison of the projected outcomes of the observed versus optimised pandemic mitigation strategy consisting of business and school closures against a background of Sinovac vaccinations for the period May to August 2021. This is to illustrate how the decision framework is used to find optimised closure strategies as background mitigation for the booster vaccination scenarios. The SC of all the configurations (assuming valuation set 2) are visualised in Figure 2. The darker shaded areas show configurations associated with higher total SC. Strategies that leave schools and businesses relatively open are associated with higher SC, explained by the high number of monetised YLLs that exceed monetised losses to education and economic output in more closed scenarios. We estimate that the actual configuration chosen by Indonesian decision makers was 10% school opening and 1.0 business closure, but the optimal configuration to minimise SC would have been 50% school opening and 3.0 business closure (light pink area). Of course, this is a theoretical assessment and it is questionable whether such stringent business closures would have been feasible.

Table 3 shows the optimal configuration chosen given each of the four valuation sets. Valuation sets 3 and 4 value education more highly, hence decisions using those sets will return configurations that lean more heavily towards keeping schools open. Valuation sets 2 and 4 value lives more highly, hence decisions using those sets will return

configurations that lean more heavily towards closing schools and businesses. Note that for all valuation sets, schools are more open, the economy is more closed, and there are fewer deaths than was actually observed in Indonesia over the period. This implies that Indonesian decision makers chose less restrictions on the economy at the expense of both lives and education and, for the range of valuations we consider, the cost of these societal losses exceeded the savings made by prioritizing the economy. Figure 3 compares SC between observed and optimised pandemic mitigation, assuming valuation set 2. An optimised configuration of business and school closures would have reduced SC by around $100 billion, by reducing deaths and educational losses at the expense of more stringent business closures. This figure also illustrates that the economic loss from worker absence due to COVID-19 is a very small part of the overall SC of the pandemic and its mitigation.

3.2   Booster vaccination scenario analysis

We now turn to the projected benefits of booster vaccinations. Configurations and summary statistics for the optimal solutions for the twelve-month period are shown in Tables 4 and 5 for each scenario, with the configurations shown graphically in Figure 4. The optimal configurations are the cost-minimising background mitigation via school and business closures that must be kept in place to contain the epidemic while booster (and Sinovac) vaccinations are scaled up. The configurations are chosen to minimise SC given valuation set 2 (results for other valuation sets given in Section D.2) amid uncertainty in epidemic transmission.

We project that an expedited booster campaign with target coverage of 80% and 187 million doses of Moderna (scenario 3) would result in an expected societal gain of $381 billion (95% confidence interval 260–640), compared to no boosters (scenario 1), see Table 5. The gain represents the societal value of the booster campaign to Indonesia in monetary terms for our central scenario assuming valuation set 2, where one person-year of education is valued at $15,000 and one life year at $80,000 (see table 2). We assume optimised mitigation via school and business closures and a constant background scale-up of 1st and 2nd vaccinations with Sinovac in both the booster and the counterfactual scenarios. We compute the gain by comparing the costs associated with optimised mitigation with booster campaigns to the counterfactual optimised mitigation without a booster campaign, assuming the social planner adopts the SC-minimising approach to background mitigation. Societal gains differ for the other valuation sets (see table 14), with a minimum gain of $366 billion ($270-$580) for valuation set 1, and a maximum gain of $609 billion ($490-$970) for valuation set 4. We find that the best-case scenarios for both booster campaigns and the no-booster counterfactual result in similar numbers of expected deaths with high variance, which is driven by high uncertainty in transmission. The societal gain from the booster vaccines is mainly realised in less stringent school and business closures required to control transmission. In-school education increases from the no-booster scenario 1 to the expedited booster scenario scenario 3 by 19 million person-years, a monetised educational gain of $189 billion. This implies that boosters reduce the pandemic education loss by 51%. The GDP gain from avoided business closures is of similar magnitude at $174 billion, meaning that boosters reduce the economic hit of the pandemic by 61%. On top of the avoided social and economic costs, the difference in the expected number of deaths is 14,000, or 300,000 YLLs, a monetised gain in life years of $18 billion. Boosters result in a reduction in deaths of about 16%.

A moderate booster campaign reaching only 40% of the target population (scenario 2) would save an expected $235 billion in SC for Indonesia, compared to a no-booster scenario 1, assuming valuation set 2. Gains increase from a minimum of $205 billion ($110-$310) to a maximum of $389 billion ($320-$610) for valuation sets 1 to 4, see table 14. For valuation set 2, educational gains are 9 million person-years of in-person education, or $92 billion. The GDP

gain is $141 billion, and the YLL saving $2 billion (1,000 averted deaths).

When expressing gains per vaccine dose of the expedited compared to the no-booster scenarios 3 vs 1, we project that the expected social benefit in the first year of booster rollout is $2,000 (95% CI 1,400–3,400) per dose for 187 million doses. This means that for every booster dose bought and administered, the return in terms of gained schooling, life years and GDP is $2,000. Gains increase from a minimum of $2,000 ($1,400-$3,100) to a maximum of $3,300 ($2,600-$5,200) for valuations 1 to 4 (see table 13).

Gains are higher when comparing the moderate compared to the no-booster scenarios 2 vs 1. We project that the expected social benefit of 93.5 million doses is $2,500 per dose in the first year assuming valuation set 2. The projected gains vary from $2,200 ($1,200-$3,300) to $4,200 ($3,400-$6,600) for valuation sets 1 to 4 (table 13). Note that there are diminishing returns to the expedited compared to moderate booster campaign: the return is around $2,500 (95% CI 1,700–3,400) per dose for coverage up to 40%, and $2,000 per dose for extending coverage to 80%.

Another way of expressing the societal gain of boosters is to translate or equate it to years of education or years of life via their valuations. The $381 billion gain is equivalent to an expected monetised gain of 25 million person-years of education, 4.8 million life years, or 410,000 lives of those aged 65 years and older.

The exact value of the societal benefit depends on the specifics of the simulation and how the SC are calculated. For example, as time passes, the reward of vaccination increases: Figure 4 suggests that returns will continue to accumulate beyond twelve months, as the booster scenarios begin the following year with more open business and schools, which is associated with additional SC gains compared to the no-booster scenario.
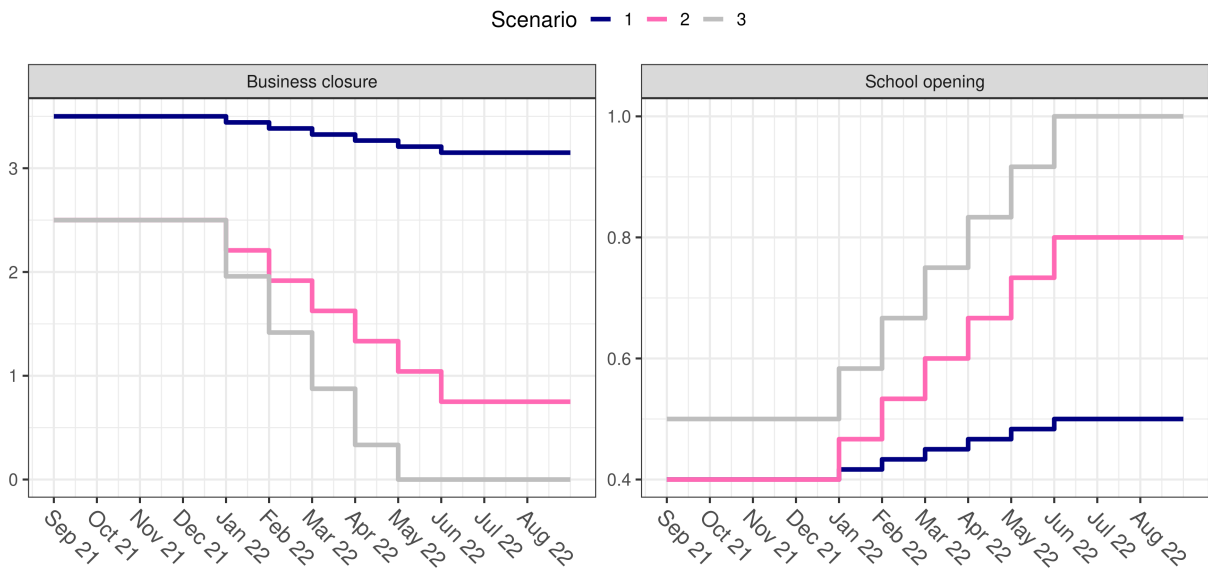

Figure 4: Optimal trajectories of mitigation via closures under three booster vaccination scenarios. Note: Scenario 1 no boosters, scenario 2 moderate booster campaign with 40% vaccination coverage at twelve months, scenario 3 expedited booster campaign with 80% vaccination coverage at twelve months. We constrain the configuration to be constant for the first four months, then allow a linear increase in opening over six months, and then fix the achieved configuration for the remaining two months of the projection horizon. Costs are evaluated for the full twelve-month period using valuation set 2. The figures show that booster vaccines allow both schools and businesses to open earlier.

Table 4: Optimal pandemic mitigation configuration for three vaccine booster rollout scenarios.

Scenario	One-year coverage, %	Doses, millions	First four months		At ten months	
			School opening, %	Business closure	School opening, %	Business closure
Scenario 1	0	0	40	3.5	50	3.15
Scenario 2	40	93.5	40	2.5	80	0.75
Scenario 3	80	187	50	2.5	100	0

The One-year coverage is the percentage of the three target groups given a booster dose by the end of the twelve-month period, and Doses is the total number of Moderna doses administered. These define the scenarios. School opening and Business closure are constant for the first four months, change linearly for the next six months, and are constant again for the final three months. Configurations are chosen to minimise socio-economic costs given the valuations $15,000 per year of education and $80,000 per year of life under uncertain epidemic transmission. Business closure is relative to the configuration observed in February 2021.

Table 5: Socio-economic costs under three vaccine booster rollout scenarios, one year projection horizon

Scenario	Person-years of educa-tion loss, in-school education[a] millions[a]	Cost of educationbillion $[b]	GDP, billion $[a]	GDP loss, billion $[b]	YLLs, millions[a]	Cost of YLL, billion $[b]	Deaths, millions[a]	Socio-economic costs, billion $[b]	Benefit per dose, $
Scenario 1	30	369	707 (707-708)	286 (285-288)	2.2 (0.14-13)	113 (7.0-650)	0.086 (0.01-0.48)	768 (661-1,310)	
Scenario 2	39	277	769 (769-770)	145 (145-147)	2.2 (0.15-12)	111 (7.4-587)	0.085 (0.01-0.44)	533 (430-1,010)	2,500 (1,700-3,400)
Scenario 3	49	180	788 (787-788)	112 (111-113)	1.9 (0.14-9.9)	95 (7.2-497)	0.072 (0.01-0.37)	387 (299-791)	2,000 (1,400-3,400)

Notes: Scenario 1 no boosters; Scenario 2 Moderna boosters with 40% coverage after 12 months; Scenario 3 Moderna boosters with 80% coverage after 12 months; Background gradual scale-down of optimised pandemic mitigation via business and school closures, and linear scale-up of 1st and 2nd doses with Sinovac are assumed; Expected values with 95% confidence intervals in parentheses.

[a] Outputs from the epidemiological model (YLLs, Deaths) and economic model (Person-years of in-school education, GDP) for the configuration

[b] Costed losses compared to the no-pandemic counterfactual, which contribute to the socio-economic costs as defined in Equation 2 using Valuation 2 from Table 2

4   Discussion

We present here an approach using the integrated epidemiological-economic model Daedalus that allows for the comprehensive evaluation of a combination strategy of pharmaceutical and non-pharmaceutical pandemic mitigation in terms of costs to the economy, to education, and to lives. These strategies are often compared in terms of deaths averted. However, most countries adopt some form of mitigation with non-pharmaceutical interventions, most notably business and school closures. This implies that vaccinations and closure strategies are complements: When vaccinations are scaled up, closures can be reduced, possibly with only small overall impact on deaths. This makes it important to evaluate the societal impact of vaccines comprehensively, and not only in terms of deaths. Our model takes such evaluations into account as part of the decision-making process. The model can be used to derive estimates of the schooling–economy–health trade-off for any mitigation strategy via comparison of the socio-economic costs.

We use SC to choose optimal configurations in a decision framework, and to estimate the expected societal benefit of vaccinations in Indonesia. Assuming a valuation of a life year of $80,000 and a valuation of a year of education of $15,000 in our central scenario, we estimate the societal benefit of two alternative booster campaigns against a no-booster counterfactual, assuming a constant scale-up of 1st and 2nd doses of the Sinovac vaccine and optimised pandemic mitigation via business and school closures. Specifically, we project benefits for 187 and 93.5 million doses of Moderna with 80% and 40% target coverage for an expedited and moderate campaign, respectively. The boosters would reduce the socio-economic costs of the pandemic to Indonesia by $381 (expedited, for moderate $235) billion over a twelve-month time horizon. This comprises of 19 (9) million gained person-years of in-person education, or monetised education gains of $189 ($92) billion; economic gains of $174 ($141) billion; and 300,000 (15,000) gained life years, or 19,000 (1,000) averted deaths, monetised health gains of $18 ($2) billion. Each Moderna booster dose is worth approximately $2,000 ($2,500) in the first year. If we assume the cost of acquisition and administration to be no more than $30 per dose (Dyer, 2021; Griffiths et al., 2021; Marriott and Maitland, 2021), the returns on investments (ROI) are at least $66 ($83) for every $ spent. If instead the cost is $14 per dose, the returns on investments (ROI) are $143 ($179) for every $ spent. This would constitute a substantial societal gain associated with booster vaccinations. The high returns are particularly astounding considering they are estimated against the background scale-up of standard vaccinations with the Sinovac vaccines.

Unlike previous projections from integrated economic-epidemiological models, we use monetary valuations of key societal benefits to make explicit the agonising trade-off that the social planner is faced with in pandemic mitigation. Particularly, we include the costs of lost education. This is highly relevant, because many countries adopted pandemic mitigation strategies involving extensive school closures, but not much is known about the long-term costs associated with a sustained loss of in-person education. A less skilled and productive workforce may result in long-term adverse consequences on countries' economic growth and welfare. Some experts believe that the loss to education will turn out to contribute a substantial fraction of the overall costs of the pandemic and its mitigation to economies (Hanushek and Woessmann, 2020). Here, we calculate short- and mid-term economic losses, and the longer-term economic losses arising from interrupted in-person education, and add them to the costs of economic closures. The decisions on business closures in our model are informed by actual observed configurations for the country, under the assumption that linear scaling is feasible. We define a grid of possible configurations and choose the optimum from among them. By discretising the solution space, we enable sampling of multiple feasible epidemic trajectories, for which the costs for all options can be evaluated. This allows us to find the optimal decision under uncertainty.

We sample trajectories because an unfolding epidemic is unpredictable by nature, and so future projections – and any metrics derived thereof – are subject to uncertainty. Our framework for prospective analyses is formulated as a decision made under uncertainty, evaluating the expected socio-economic costs given the uncertain parameters, and describing the uncertainties using probability distributions that reflect beliefs about what values the parameters are likely to take. Here, for transmission, we have sampled values that have been inferred for previous months. Values could be chosen (or adjusted) instead to reflect planned mitigation, changes in expected compliance, or random changes to the circulating virus profile. The same principle can be applied to other parameters about which we might be uncertain, such as vaccine effects. Identifying the optimal decision under uncertainty also returns a distribution over likely epidemic trajectories: these provide benchmarks against which the unfolding epidemic trajectory can be assessed.

Decisions made considering a short time period are misleading because they may burden the following period with substantial costs (shown in Appendix D.1). The optimal decision chosen for a short period will likely leave the next period with high and rising cases, hospitalisations and deaths. Therefore, the choices should be tested in longer simulations, or with the cost of the following period also taken into account (as in Section 2.3.1).

4.1   Limitations

We make a number of simplifying assumptions about the relationships between education, economic closures and health outcomes. Incorporating more nuanced relationships is part of ongoing work. We do not adjust the valuations of life years or years of education, which are related variously to GDP, Gross National Income, or wage differentials, according to changes in expected output. Instead we use pre-pandemic values for their computation. Our evaluation relies on costing years of life, years of education, and economic activity in a common currency. There are not objective values, in any currency, at which a year of life or a year of education *should* be valued. A range of plausible values can be generated and tested in retrospective analyses, asking "what would have happened if we had chosen to minimise the socio-economic costs given these valuations", in order to evaluate the preferences of the social planner regarding the resulting counterfactual epidemic curves. For the purposes of illustration, we explored the sensitivity of our results to four alternative valuation sets.

It is possible that our costings of education and health are conservative. For example, school closures disproportionately disadvantage students who are female (Akmal et al., 2020) or belong to lower-income households (Jang and Yum, 2020; Azevedo et al., 2020; Engzell et al., 2021; Fuchs-Schündeln et al., 2020), but the societal costs associated with increased gender and income related educational inequalities is not considered in our calculations. Additionally, the cost function does not include the cost of increased probability of student dropout associated with extended closures (potentially affecting 2% of students (Purnamasari and Ali, 2021)). Finally, we do not consider that attendance of students from poorer households may suffer due to reduced availability of funds for tuition. This problem may affect up to a third of students (Purnamasari and Ali, 2021), and it increases with stringency of business closures.

There are other costs we have not included here, including the impact of COVID-19-driven life-long disability on long-term workforce productivity, the societal cost of disability for a person of any age, or the cost of lives lost due to deferred medical care for other conditions. Moreover, we have not included the differential effect of economic closures to different groups, in particular different socio-economic groups, and the resulting increase in income inequality and its associated costs for the society (Sawada and Sumulong, 2021; Surendra et al., 2021). We

therefore believe that our calculations of socio-economic costs may be conservative estimates of the true costs. It is straightforward to adjust our findings in the light of new and improved evidence on monetary valuations.

For the evaluation of the cost of economic loss, we assumed that the size of the GVA shortfall has no effect on long-term growth (i.e. the extent of persistent damage): we assumed that the IMF-estimated GDP path would be rejoined in the year 2026. This assumption will be more plausible for small losses than for large ones, and for large, slow-growing economies than for fast-growing emerging economies (Slater, 2020; Barrett et al., 2021). As more evidence on economic impacts becomes available, these can readily be incorporated into our model.

We have used a deterministic model for the epidemic, which does not include feedback between the epidemic and population behaviour. The large decline in transmission observed in the months of July and August 2021 was likely due to the high numbers of people being infected, and the population responding by taking additional precautions (Perrotta et al., 2021), which in turn would reduce transmission. In our counterfactual simulations, we assume the same drop in transmission, which may be unjustified for scenarios where hospital occupancy does not reach such a high level.

We have made some crude assumptions for school opening. Assumptions around the contact rates between school-age people, the community and the economic sectors are crude, and our findings are likely sensitive to misspecification of contact rates. Our calibration to Indonesia was also limited by available economic data, in particular, difficulties in measuring the economic output of the informal economy in national accounts (Alon et al., 2020).

4.2 Policy insights

Despite the limitations, our model can be used to prepare Indonesia and other countries for the next phase of the pandemic. It is to be expected that the question of booster vaccinations will dominate pandemic mitigation strategies in 2022 and beyond. It is well established that both naturally acquired and vaccine-induced immunity wane over time. Although evidence is still inconclusive regarding the rate of waning, it is relatively uncontroversial that it is to be measured in months rather than years. Moreover, many LMICs have insufficient coverage of 1st and 2nd dose vaccinations, and relied heavily on vaccines with a less favourable vaccine protection profile, such as Sinovac. Finally, the constant threat of variants emerging, such as the most recent Omicron variant, erodes further the vaccine protection achieved so far against infection, onward transmission, severe disease and deaths.

This means that smart mitigation strategies that combine pharmaceutical and non-pharmaceutical interventions will preoccupy public health policy making for the foreseeable future. Optimisation approaches such as the one used here provide actionable quantitative evidence to policy makers. They are a tool for evaluating the scope for benefits (and costs!) yielded by different policy options, and they can measure the impact of incremental policy changes holding other factors unaltered. Optimisation approaches allow policy makers to adopt an encompassing perspective on a decision problem that acknowledges that global objectives, constraints and guidelines have to be combined to take decisions. We have combined three global objectives that stand in conflict with each other during pandemic mitigation, and converted them into the same metric. While this is associated with obvious limitations, it has the great advantage that it simplifies the complex decision problem. Identifying optimal configurations under uncertainty allows us to evaluate the benefit of vaccination rollout strategies by comparing the smallest expected costs for each. The evaluation rests on the values given to years of life and years of education; therefore, the saving

can be translated back into these terms.

Our modelling approach is designed to help decision makers around the world to make informed decisions on complex combination mitigation strategies, and equip them with the tools that help them to minimise deaths, and the economic and social costs of the pandemic.

5   Acknowledgements

Author contribution

RJ, DH, PD, GF, MP, PS and KH conceived and designed the work; RJ undertook the analysis and interpretation of data; BD, DH and PD contributed to the analysis of data; BD, GF, MP, PS, and KH contributed to the interpretation of data; RJ, DH and PD created new software used in the work; RJ and KH wrote the first draft of the paper and DH, PD, GF and PS substantially revised it. All authors have approved the submitted version and have agreed to be personally accountable for the author's own contributions and to ensure that questions related to the accuracy or integrity of any part of the work, even ones in which the author was not personally involved, are appropriately investigated, resolved, and the resolution documented in the literature.

6   References

Akmal, M., Hares, S. and O'Donnell, M. (2020), Gendered impacts of COVID-19 school closures: Insights from frontline organisations, Technical report, Center for Global Development.

Alon, T. M., Kim, M., Lagakos, D. and Vuren, M. V. (2020), How should policy responses to the Covid-19 pandemic differ in the developing world?, Technical report, National Bureau of Economic Research.

Ananthapavan, J., Moodie, M., Milat, A. J. and Carter, R. (2021), 'Systematic review to update 'value of a statistical life' estimates for Australia', *International Journal of Environmental Research and Public Health* **18**(11).

Andrews, N., Stowe, J., Kirsebom, F., Toffa, S., Rickeard, T., Gallagher, E., Gower, C., Kall, M., Groves, N., O'Connell, A.-M., Simons, D., Blomquist, P. B., Zaidi, A., Nash, S., Iwani Binti Abdul Aziz, N., Thelwall, S., Dabrera, G., Myers, R., Amirthalingam, G., Gharbia, S., Barrett, J. C., Elson, R., Ladhani, S. N., Ferguson, N., Zambon, M., Campbell, C. N., Brown, K., Hopkins, S., Chand, M., Ramsay, M. and Lopez Bernal, J. (2021), 'Effectiveness of COVID-19 vaccines against the Omicron (B.1.1.529) variant of concern', *medRxiv* .

Azevedo, J. P., Hasan, A., Goldemberg, D., Aroob, S. and Koen Geven, I. (2020), Simulating the potential impacts of COVID-19 school closures on schooling and learning outcomes, Technical report, World Bank Group.
URL: *http://www.worldbank.org/prwp.*

Barrett, P., Das, S., Magistretti, G., Pugacheva, E. and Wingender, P. (2021), After-effects of the COVID-19 pandemic: Prospects for medium-term economic damage, Technical Report 203, International Monetary Fund.

Béraud, G., Kazmerciak, S., Beutels, P., Levy-Bruhl, D., Lenne, X., Mielcarek, N., Yazdanpanah, Y., Boëlle, P. Y., Hens, N. and Dervaux, B. (2015), 'The French connection: The first large population-based contact survey in France relevant for the spread of infectious diseases', *PLoS ONE* **10**(7), 1–22.

Bloom, D. E., Kuhn, M. and Prettner, K. (2020), Modern infectious diseases: Macroeconomic impacts and policy responses, Technical report, National Bureau of Economic Research.

Briggs, A., Claxton, K. and Sculpher, M. (2006), *Decision Modelling for Health Economic Evaluation*, OUP UK.

Byambasuren, O., Cardona, M., Bell, K., Clark, J., McLaws, M. L. and Glasziou, P. (2020), 'Estimating the extent of asymptomatic COVID-19 and its potential for community transmission: Systematic review and meta-analysis', *Journal of the Association of Medical Microbiology and Infectious Disease Canada* **5**(4), 223–234.

Cobb, C. W. and Douglas, P. H. (1928), 'Theory of production', *American Economic Association* pp. 139–165.

Cutler, D. M. and Summers, L. H. (2020), 'The COVID-19 pandemic and the $16 trillion virus', *JAMA* **324**(15).

Djaafara, B. A., Whittaker, C., Watson, O. J., Verity, R., Brazeau, N. F., Widyastuti, Oktavia, D., Adrian, V., Salama, N., Bhatia, S., Nouvellet, P., Sherrard-Smith, E., Churcher, T. S., Surendra, H., Lina, R. N., Ekawati, L. L., Lestari, K. D., Andrianto, A., Thwaites, G., Baird, J. K., Ghani, A. C., Elyazar, I. R. and Walker, P. G. (2021), 'Using syndromic measures of mortality to capture the dynamics of COVID-19 in Java, Indonesia, in the context of vaccination rollout', *BMC Medicine* **19**(1), 1–13.

Dyer, O. (2021), 'Covid-19: Countries are learning what others paid for vaccines', *BMJ* **372**(281).

Engzell, P., Frey, A. and Verhagen, M. D. (2021), 'Learning loss due to school closures during the COVID-19 pandemic', *Proceedings of the National Academy of Sciences of the United States of America* **118**(17).

Eyre, D. W., Taylor, D., Purver, M., Chapman, D., Fowler, T., Pouwels, K. B., Walker, A. S. and Peto, T. E. A. (2022), 'Effect of Covid-19 vaccination on transmission of Alpha and Delta variants', *The New England Journal of Medicine* pp. 1–13.
URL: *http://www.ncbi.nlm.nih.gov/pubmed/34986294*

Feenstra, R. C., Inklaar, R. and Timmer, M. P. (2015), 'The Next Generation of the Penn World Table', *American Economic Review* **105**(10), 3150–3182.
URL: *www.ggdc.net/pwt*

Ferguson, N., Ghani, A., Cori, A., Hogan, A., Hinsley, W. and Volz, E. (2021), Report 49: Growth, population distribution and immune escape of Omicron in England, Technical report, Imperial College London COVID-19 Response Team.

Ferguson, N., Ghani, A., Hinsley, W. and Volz, E. (2021), Report 50: Hospitalisation risk for Omicron cases in England, Technical Report December, Imperial College London COVID Response Team, London.
URL: *https://www.imperial.ac.uk/media/imperial-college/medicine/mrc-gida/2021-12-22-COVID19-Report-50.pdf*

Fernald, J., Li, H. and Ochse, M. (2021), 'Future output loss from COVID-induced school closures', *Federal Reserve Bank of San Francisco Economic Letter* .
URL: *https://www.frbsf.org/economic-research/publications/economic-letter/2021/february/future-output-loss-from-covid-induced-school-closures/*

Fuchs-Schündeln, N., Krueger, D., Ludwig, A. and Popova, I. (2020), The long-term distributional and welfare effects of Covid-19 school closures, Technical report, National Bureau of Economic Research.

Global Burden of Disease Collaborative Network (2021), Global Burden of Disease Study 2019 (GBD 2019) Reference Life Table, Technical report, Institute for Health Metrics and Evaluation (IHME), Seattle, United States of America.

Griffiths, U., Adjagba, A., Attaran, M., Hutubessy, R., Van De Maele, N., Yeung, K., Aun, W., Cronin, A., Allan, S., Brenzel, L., Resch, S., Portnoy, A., Boonstoppel, L., Banks, C. and Alkenbrack, S. (2021), Costs of delivering COVID-19 vaccine in 92 AMC countries, Technical Report February, COVAX Working Group.
URL: *https://www.who.int/publications/i/item/10665337553*

Hammitt, J. K. (2020), 'Valuing mortality risk in the time of COVID-19', *Journal of Risk and Uncertainty* **61**(2), 129–154.

Hanushek, E. A. and Woessmann, L. (2020), The economic impacts of learning losses, Technical report, OECD.

Haw, D., Forchini, G., Christen, P., Bajaj, S., Hogan, A. B., Winskill, P., Miraldo, M., White, P. J., Ghani, A. C., Ferguson, N. M., Smith, P. C. and Hauck, K. (2020), Report 35: How can we keep schools and universities open? Differentiating closures by economic sector to optimize social and economic activity while containing SARS-CoV-2 transmission, Technical report, Imperial College London COVID Response Team.
URL: *https://www.imperial.ac.uk/mrc-global-infectious-disease-analysis/covid-19/report-35-schools/*

Inklaar, R. and Timmer, M. (2013), Capital, Labor and TFP in PWT8. 0, Technical report, University of Groningen.
URL: *http://piketty.pse.ens.fr/files/InklaarTimmer13.pdf*

International Monetary Fund (2021*a*), World Economic Outlook: Managing Divergent Recoveries, Technical report, International Monetary Fund.

International Monetary Fund (2021*b*), World Economic Outlook: Recovery During a Pandemic, Technical Report October, International Monetary Fund.

Jackson, C., Johnson, R., De Nazelle, A., Goel, R., De Sá, T. H., Tainio, M. and Woodcock, J. (2021), 'A guide to value of information methods for prioritising research in health impact modelling', *Epidemiologic Methods* **10**(1), 1–22.

Jang, Y. and Yum, M. (2020), Aggregate and intergenerational implications of school closures: A quantitative assessment, Technical report, Shanghai University of Finance and Economics.

Jara, A., Undurraga, E. A., González, C., Paredes, F., Fontecilla, T., Jara, G., Pizarro, A., Acevedo, J., Leo, K., Leon, F., Sans, C., Leighton, P., Suárez, P., García-Escorza, H. and Araos, R. (2021), 'Effectiveness of an inactivated SARS-CoV-2 vaccine in Chile', *New England Journal of Medicine* **385**(10), 875–884.

Jara, A., Undurraga, E. A., Zubizarreta, J. R., González, C., Pizarro, A., Acevedo, J., Leo, K., Paredes, F., Tomas, B., Veronica, V., Marcelo, M., Leon, F., Ignacio, P., Leighton, P., Suárez, P., Juan, C. R., García-Escorza, H. and Araos, R. (2022), 'Effectiveness of homologous and heterologous booster shots for an inactivated SARS-CoV-2 vaccine: A large-scale observational study', *Under Review* .
URL: *http://dx.doi.org/10.2139/ssrn.4005130*

Jordà, Ò., Singh, S. R. and Taylor, A. M. (2020), Longer-run economic consequences of pandemics, Technical report, Federal Reserve Bank of San Francisco.
URL: *https://www.frbsf.org/economic-research/files/wp2020-09.pdf*

K. J. Arrow, H. B. Chenery, B. S. M. and Solow, R. M. (1961), 'Capital-labor substitution and economic efficiency', *The Review of Economics and Statistics* **43**, 222–250.

Knock, E. S., Whittles, L. K., Lees, J. A., Perez-Guzman, P. N., Verity, R., FitzJohn, R. G., Gaythorpe, K. A., Imai, N., Hinsley, W., Okell, L. C., Rosello, A., Kantas, N., Walters, C. E., Bhatia, S., Watson, O. J., Whittaker, C., Cattarino, L., Boonyasiri, A., Djaafara, B. A., Fraser, K., Fu, H., Wang, H., Xi, X., Donnelly, C. A., Jauneikaite, E., Laydon, D. J., White, P. J., Ghani, A. C., Ferguson, N. M., Cori, A. and Baguelin, M. (2021), 'Key epidemiological drivers and impact of interventions in the 2020 SARS-CoV-2 epidemic in England', *Science translational medicine* **13**.

Marriott, A. and Maitland, A. (2021), The Great Vaccine Robbery, Technical report, The People's Vaccine.

Meslé, M. M., Brown, J., Mook, P., Hagan, J., Pastore, R., Bundle, N., Spiteri, G., Ravasi, G., Nicolay, N., Andrews, N., Dykhanovska, T., Mossong, J., Sadkowska-Todys, M., Nikiforova, R., Riccardo, F., Meijerink, H., Mazagatos, C., Kyncl, J., McMenamin, J., Melillo, T., Kaoustou, S., Lévy-Bruhl, D., Haarhuis, F., Rich, R., Kall, M., Nitzan, D., Smallwood, C. and Pebody, R. G. (2021), 'Estimated number of deaths directly averted in people 60 years and older as a result of COVID-19 vaccination in the WHO European Region, December 2020 to November 2021', *Eurosurveillance* **26**(47).
URL: *http://dx.doi.org/10.2807/1560-7917.ES.2021.26.47.2101021*

National Economic and Development Authority (2021), COVID-19 pandemic to cost PHP 41.4 T for the next 40 years, Technical report, National Economic and Development Authority.
URL: *https://neda.gov.ph/covid-19-pandemic-to-cost-php-41-4-t-for-the-next-40-years-neda/*

Pan, H. X., Liu, J. K., Huang, B. Y., Li, G. F., Chang, X. Y., Liu, Y. F., Wang, W. L., Chu, K., Hu, J. L., Li, J. X., Zhu, D. D., Wu, J. L., Xu, X. Y., Zhang, L., Wang, M., Tan, W. J., Huang, W. J. and Zhu, F. C. (2021), 'Immunogenicity and safety of a severe acute respiratory syndrome coronavirus 2 inactivated vaccine in healthy adults: Randomized, double-blind, and placebo-controlled phase 1 and phase 2 clinical trials', *Chinese Medical Journal* **134**(11), 1289–1298.

Perrotta, D., Grow, A., Rampazzo, F., Cimentada, J., Del Fava, E., Gil-Clavel, S. and Zagheni, E. (2021), 'Behaviours and attitudes in response to the COVID-19 pandemic: insights from a cross-national Facebook survey', *EPJ Data Science* **10**(1), 1–13.
URL: *http://dx.doi.org/10.1140/epjds/s13688-021-00270-1*

Prem, K., Cook, A. R. and Jit, M. (2017), 'Projecting social contact matrices in 152 countries using contact surveys and demographic data', *PLoS Computational Biology* **13**(9), e1005697.
URL: *https://doi.org/ 10.1371/journal.pcbi.1005697*

Purnamasari, R. S. and Ali, R. (2021), Education services during the COVID-19 pandemic: Indonesia COVID-19 Observatory Brief, Technical Report 8, The World Bank, Washington, DC.
URL: *https://openknowledge.worldbank.org/handle/10986/35125*

Robinson, L. A., Hammitt, J. K. and O'Keeffe, L. (2019), 'Valuing mortality risk reductions in global benefit-cost analysis', *Journal of Benefit-Cost Analysis* **10**, 15–50.

Robinson, L. A., Sullivan, R. and Shogren, J. F. (2021), 'Do the benefits of COVID-19 policies exceed the costs? Exploring uncertainties in the age–VSL relationship', *Risk Analysis* **41**(5), 761–770.

Rosenberg, E., Dorabwila, V., Easton, D., Bauer, U., Kumar, J., Hoen, R., Hoefer, D., Wu, M., Lutterloh, E., Conroy, M. B., Greene, D. and Zucker, H. A. (2021), 'Covid-19 vaccine effectiveness in New York State', *New England Journal of Medicine* **386**.

Sawada, Y. and Sumulong, L. (2021), ADBI Working Paper 1251: Macroeconomic impact of COVID-19 in developing Asia, Technical Report 1251, Asian Development Bank Institute, Tokyo.
URL: *https://www.adb.org/publications/macroeconomic-impact-covid-19-developing-asia*

Shu, Y. and McCauley, J. (2017), 'GISAID: Global initiative on sharing all influenza data – from vision to reality', *Eurosurveillance* **22**(13), 2–4.

Slater, A. (2020), 'After the pandemic: Medium-term growth uncertainties', *Economic Outlook* **44**(2), 5–9.

Surendra, H., Salama, N., Lestari, K. D., Adrian, V., Widyastuti, Oktavia, D., Lina, R. N., Djaafara, B. A., Fadilah, I., Sagara, R., Ekawati, L. L., Nurhasim, A., Ahmad, R. A., Kekalih, A., Syam, A. F., Shankar, A. H., Thwaites, G., Baird, J. K., Hamers, R. L. and Elyazar, I. R. (2021), 'Pandemic inequity in a megacity: a multilevel analysis of individual, community and health care vulnerability risks for COVID-19 mortality in Jakarta, Indonesia', *medRxiv* .

The World Bank, UNICEF and UNESCO (2021), The State of the Global Education Crisis: A Path to Recovery, Technical report, The World Bank, UNICEF, and UNESCO, Washington D.C., Paris, New York.

UN Economic and Social Affairs (2008), *International Standard Industrial Classification of All Economic Activities Revision 4*, United Nations, New York.

Wulandari, L. (2020), Deriving Indonesia's value of a statistical life, Technical report, University of Toronto.
   URL: *https://laidlawscholars.network/documents/deriving-indonesia-s-vsl*

Xia, F., Yang, X., Cheke, R. A. and Xiao, Y. (2021), 'Quantifying competitive advantages of mutant strains in a population involving importation and mass vaccination rollout', *Infectious Disease Modelling* **6**, 988–996.
   URL: *https://doi.org/10.1016/j.idm.2021.08.001*

Yarrow, N., Masood, E. and Afkar, R. (2020), Estimates of COVID-19 impacts on learning and earning in Indonesia: how to turn the tide, Technical Report August, The World Bank.
   URL: *https://openknowledge.worldbank.org/bitstream/handle/10986/34378/Main-Report.pdf*

7   Supplementary material

A   Summary of inputs

A.1   Population

Population counts from OECD are collapsed into four age groups (Table 6). The working-age population is split into those working and those not. Here, 22.7 % of the working-age population are modelled as not part of the workforce.

Table 6: Population numbers

Group	Population
0 to 4	22,002,900
5 to 19	66,580,900
20 to 64, economically inactive	34,668,600
65 to 120	14,503,100
20 to 64, economically active	152,501,300

We take remaining life expectancies from the GBD Study for the year 2019 (IHME, 2020; http://ghdx.healthdata.org/gbd-results-tool). We map the remaining life expectancy l_a for these age groups a to l_g for the model groups g as a population-weighted average:

$$l_g = \frac{\sum_{a \in g} N_a l_a}{\sum_{a \in g} N_a}.$$

A.2   The economy

Table 7 summarises the inputs for the 36 ISIC (Rev 4) Sectors for Indonesia. "Workforce" (from Trade In Employment, OECD 2015) and "GVA" (gross value added per month, from OECD, 2015) are specific to Indonesia. We assume the workforce includes those in informal employment, as informal employment was estimated at around 45% in 2014 (OECD). Values shown for the percentage able to work from home are mapped from values derived for Sri Lanka's 35 sectors (unpublished work) onto Indonesia's 36 sectors. Similarly, contact rates B and C are extrapolated from Béraud et al. (2015) assuming the UK distribution of workforce across sectors in mapping from 64 to 36.

Table 7: Summary statistics by sector

Sector	Workforce	GVA per month	Percent of staff who can work from home	Within-sector contacts	Worker-consumer contacts	Minimum opening, %
D01T03: Agriculture, forestry and fishing	38,936,600	9,601	0.1	0.5	0.0	100

D05T06: Mining and extraction of energy producing products	736,200 3,792	0.5	3.5	0.5	64
D07T08: Mining and quarrying of non-energy producing products	331,700 1,296	0.5	3.5	0.5	100
D09: Mining support service activities	297,100 353	0.5	3.5	0.5	92
D10T12: Food products, beverages and tobacco	3,891,300 4,664	7.9	3.5	0.5	100
D13T15: Textiles, wearing apparel, leather and related products	4,653,100 1,054	2.0	3.5	0.5	36
D16: Wood and products of wood and cork	748,200 481	0.4	3.5	0.5	80
D17T18: Paper products and printing	577,900 542	8.0	3.5	0.5	96
D19: Coke and refined petroleum products	22,400 1,977	0.0	3.5	0.5	60
D20T21: Chemicals and pharmaceutical products	775,600 1,295	3.7	3.5	0.5	100
D22: Rubber and plastic products	1,364,300 530	7.7	3.5	0.5	80
D23: Other non-metallic mineral products	573,800 515	5.8	3.5	0.5	60
D24: Basic metals	212,000 556	0.4	3.5	0.5	100
D25: Fabricated metal products	480,600 425	0.4	3.5	0.5	72
D26: Computer, electronic and optical products	475,100 701	13.0	3.5	0.5	72
D27: Electrical equipment	320,300 274	13.0	3.5	0.5	72
D28: Machinery and equipment, nec	217,300 230	7.5	3.5	0.5	68
D29: Motor vehicles, trailers and semi-trailers	454,200 1,311	3.4	3.5	0.5	12
D30: Other transport equipment	317,200 50	3.4	3.5	0.5	12
D31T33: Other manufacturing; repair and installation of machinery and equipment	1,068,000 239	2.3	3.5	0.5	88
D35T39: Electricity, gas, water supply, sewerage, waste and remediation services	490,900 1,017	7.0	3.5	0.5	88
D41T43: Construction	7,961,200 7,264	5.4	1.0	1.0	84
D45T47: Wholesale and retail trade; repair of motor vehicles	21,955,100 9,475	6.7	0.8	15.0	84
D49T53: Transportation and storage	4,622,700 3,574	8.1	0.8	15.0	16

D55T56: Accommodation and food services	5,166,900	2,108	3.3	0.8	15.0	48
D58T60: Publishing, audiovisual and broadcasting activities	157,300	481	37.3	2.0	2.0	100
D61: Telecommunications	343,200	1,838	37.3	2.0	2.0	100
D62T63: IT and other information services	74,400	187	22.1	2.0	2.0	100
D64T66: Financial and insurance activities	1,735,700	2,870	38.0	3.8	6.5	100
D68: Real estate activities	292,200	2,022	3.6	3.8	6.5	100
D69T82: Other business sector services	1,467,500	1,174	22.1	2.0	3.0	72
D84: Public admin. and defence; compulsory social security	4,034,000	2,779	15.9	0.0	30.0	96
D85: Education	5,748,700	2,395	25.7	0.0	30.0	10
D86T88: Human health and social work	1,505,500	759	4.3	0.0	30.0	100
D90T96: Arts, entertainment, recreation and other service activities	5,151,500	1,534	13.4	1.5	1.0	76
D97T98: Private households with employed persons	673,000	116	3.5	1.5	1.0	76

Quarterly values of GVA per sector curated and published by the national bank (https://www.bps.go.id/indicator/11/65/1/-2010-version-gdp-at-2010-version.html) are extrapolated to monthly values using Google mobility data (https://www.google.com/covid19/mobility/) for the period covering the pandemic to the end of August 2021. These values represent the extent to which was each sector open in each month, expressed as a percentage of its maximum opening, where the maximum corresponds to their output in 2019 (Figure 5). For schools, which closed in March 2020 and had not re-opened as of August 2021, we set a value of 0.55 for March 2020 and 0.1 for all months from April 2020 onward for the epidemiological model (Purnamasari and Ali, 2021).

We assume a nonlinear relationship between sector output and sector workforce. Specifically, we assume that a Cobb-Douglas function describes the change in output as a function of the change in labour (here, number of person–hours of labour). In using the Cobb-Douglas function, we are assuming constant returns to scale (Cobb and Douglas, 1928; Feenstra et al., 2015), and that capital compensates perfectly for labour shortage (K. J. Arrow, H. B. Chenery and Solow, 1961). To parametrise the model, we assume that output elasticity of labour can be approximated by the labour share of GDP, as in Inklaar and Timmer (2013). For this value (α), we use the the labour share of productivity for the year 2019 (Feenstra et al., 2015). For scenario modelling, we assume that capital and total-factor productivity do not change. Substitution by capital allows for sub-linear scaling between sector output and workforce, e.g. less than half the workforce can produce half the sector's outputs. We apply the same α value to all sectors. I.e., if the ith sector's output was valued at $x_{i,\tau}$ for month τ, we expect that the attending workforce was $w_{i,\tau} = x_{i,\tau}^{1/\alpha}$. We use the set $\{x_{i,\tau}\}$ for the computation of the sector's contribution to the economy, and both sets $\{x_{i,\tau}\}$ and $\{w_{i,\tau}\}$ for the sector's interactions with other groups in the epidemiological model. For the education
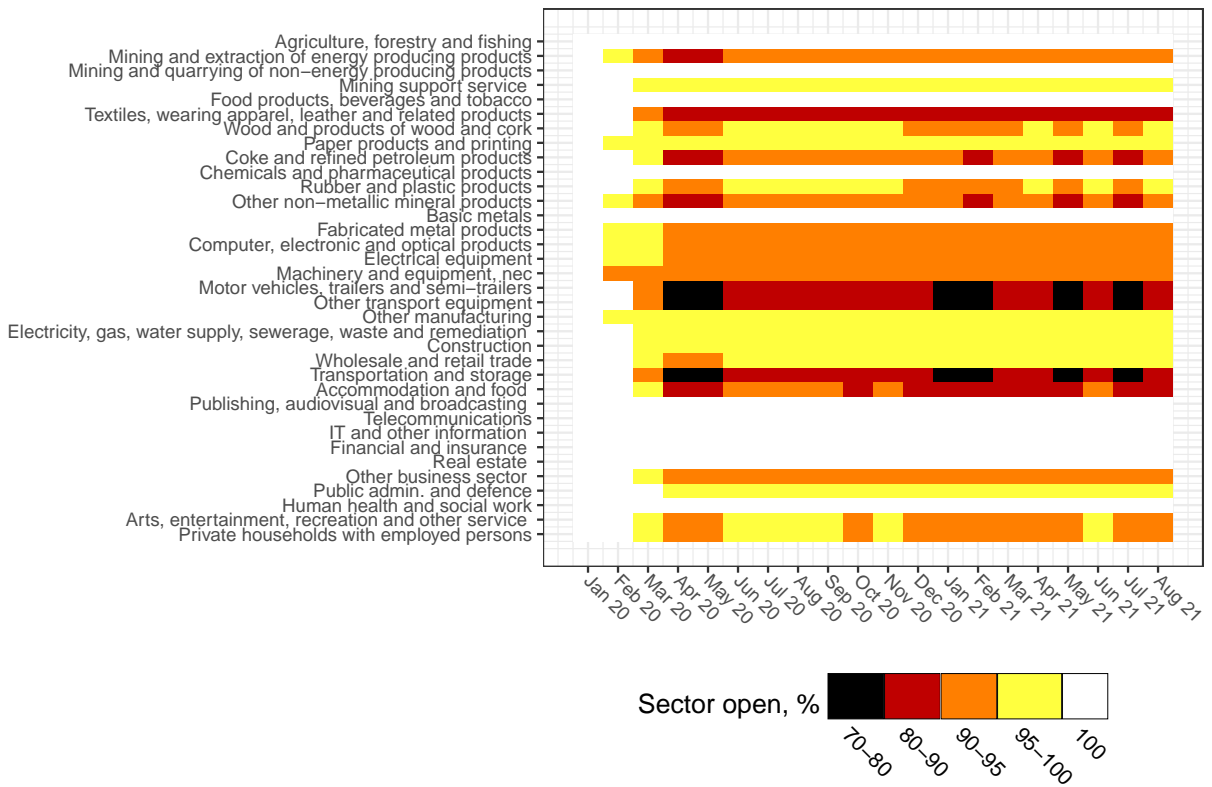
Figure 5: Estimated $x_{-33,\tau}$ for the period January 2020 to August 2021.

sector, we set $w_{33,\tau} = x_{33,\tau}$, to model a change in location (remote learning) rather than a change in productivity.

A.3   Epidemiological data

A.3.1   Hospitalisations and deaths

To fit the model, we use publicly available hospital occupancy and deaths data (https://vaksin.kemkes.go.id/#/scprovinsi).

A.3.2   Variants

From the GISAID database (Shu and McCauley, 2017), we see that the surge in cases in May to August consisted primarily of the Delta variant (B.1.617.2) and that the Alpha variant (B.1.1.7) was not the predominant strain before (Figure 6).
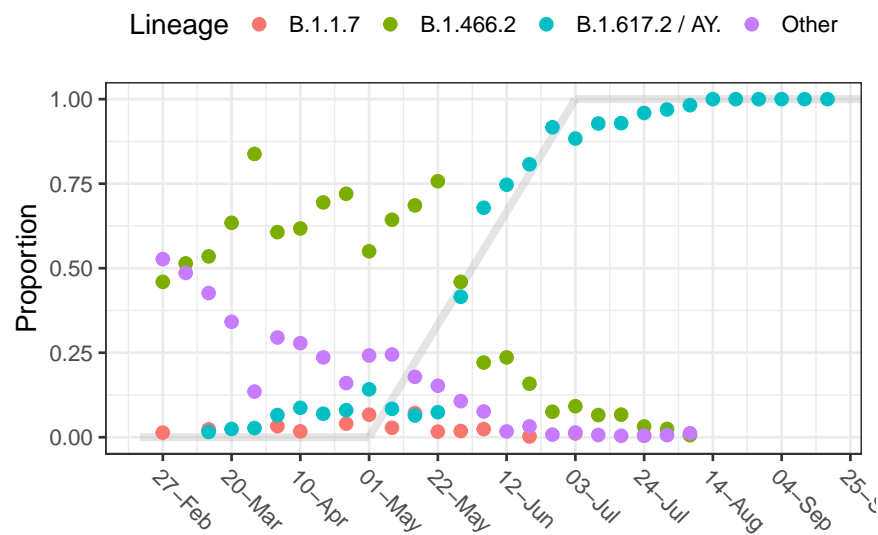

Figure 6: Lineage proportions over time.

In the model, we fit the transmission advantage and increased rates of hospitalisation and death given hospitalisation associated with the Delta variant relative to the background using a linear interpolation from 0% to 100%.

A.3.3   Vaccinations

We model vaccine administration using a series of average rates. We define each month to be a distinct time period and compute the average rate for each, using data from https://vaksin.kemkes.go.id/#/vaccines (Figure 7).

We count second vaccines doses, most of which have been Sinovac up to now, and Moderna booster shots, which were administered recently to health workers.

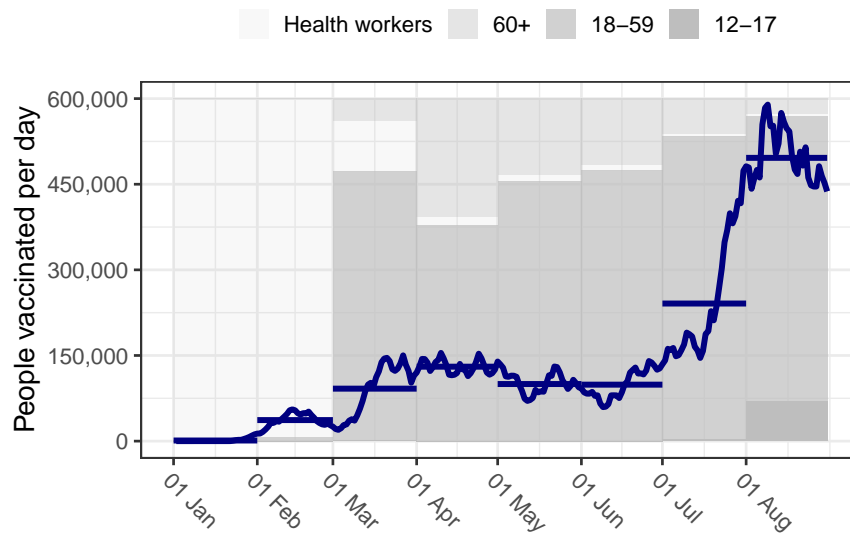We use the values given in Table 8 to model vaccine effects.

Figure 7: Vaccine administration over time.

A.3.4 Other parameters

Parameters for the model are given in Table 9, where the value "Parameters" corresponds to the label in the code (Haw et al., 2020). Contact scalars are summaries of the country-specific contact matrices for the relevant age groups and locations, from Prem et al. (2017). E.g. for contact matrix A (contacts between age groups in community settings (Haw et al., 2020)), populations N and ages i and j:

$$\text{schoolA2} = \frac{\sum_{i=2}^{4} N_i \sum_{j=2}^{4} A_{ij}}{\sum_{i=2}^{4} N_i}.$$

Table 9: Fixed parameters

Parameter	Value	Description	Source
schoolA1	0.32	Contact scalar for 0-4	Prem et al. (2017)
schoolA2	7.21	Contact scalar for 5-19	Prem et al. (2017)
travelA3	4.17	Contact scalar for work travel	Prem et al. (2017)
hospA2	0.50	Hospitality engagement scalar for age group 2	Béraud et al. (2015)
hospA3	1.00	Hospitality engagement scalar for age group 3	Béraud et al. (2015)
hospA4	1.50	Hospitality engagement scalar for age group 4	Béraud et al. (2015)
comm	3.14	Contact scalar for the community	Prem et al. (2017)

alpha	0.46	Workforce elasticity	Feenstra et al. (2015)
Thd	15.87	Expected time to death in hospital	Djaafara et al. (2021)
Threc	15.87	Expected time to recovery in hospital	Djaafara et al. (2021)
Hmax	90000.00	Hospital threshold for higher hospital fatality rate	Model choice
Delta_start	2021-04-29	Time at which Delta-variant sweep begins	Shu and McCauley (2017)
Delta_end	2021-06-28	Time at which Delta-variant sweep ends	Shu and McCauley (2017)
red	0.58	Reduced infectiousness for asymptomatic infectious	Byambasuren et al. (2020)
Text	4.60	Incubation period	Knock et al. (2021)
p1	0.60	Probability to be symptomatic	Knock et al. (2021)
Tsh	4.50	Expected time to hospital for symptomatic infection	Knock et al. (2021)
Ts	4.00	Expected time to recovery for symptomatic infection	Knock et al. (2021)
Ta	2.10	Expected time to recovery from asymptomatic infection	Knock et al. (2021)
Ti	365.00	Expected time to loss of infection-acquired immunity	Knock et al. (2021)
p3	0.10	Proportion of asymptomatic person-days spent self-isolating	Model choice
p4	0.50	Proportion of symptomatic person-days spent self-isolating	Model choice
Delta_rate	0.49	Relative transmission advantage of Delta variant	Xia et al. (2021)

B   Model description

B.1   State transitions

Possible transitions between disease states are shown in Figure 8. Transition rates are functions of time t, vaccination status v, and group identity g (where the groups are the 36 sectors and the four age groups).

The rate of infection of susceptible individuals, $k_1(v, t)$, is defined as

$$k_0(t) = (1 + p_\Delta(t)\beta_\Delta)\rho(t)\beta\left(D \cdot I^{(eff)}\right),$$

$$k_1(v, t) = f_A(v, \eta_A, t)k_0(t) \tag{12}$$

with

$$I^{(eff)} = \epsilon(1 - p_3)I_{A,0} + (1 - p_4)I_{S,0} + f_T(\eta_T, t)(\epsilon(1 - p_3)I_{A,1} + (1 - p_4)I_{S,1}).$$

Here, f_A and f_T are the reduction in acquisition and infectiousness, respectively, among the vaccinated, and η_A and η_T are the initial vaccine effect sizes; $p_\Delta(t)$ is the proportion of lineages of the Delta type and β_Δ its proportional increase in transmissibility; $\rho(t)$ is the time-dependent modifier of the rate of infection, β; D is the contact matrix

Table 8: Vaccine parameters. Parameters for Acquisition, Symptomatic given infection, Hospitalisation given symptomatic, Death given hospitalisation, and expected time to seroconversion come from Jara et al. (2022), where there are estimates both for double-dose Sinovac effects and for Pfizer boosters to a double-dose Sinovac baseline, which we use as a proxy for Moderna boosters. (Note that the study, using the methodology of Jara et al. (2021), found higher Pfizer effects for protection against infection than for those against hospitalisation and death. Therefore, we set these conditional effects to zero.) The expected lifetime for Sinovac comes from Pan et al. (2021), such that the rate of waning is its reciprocal. The expected lifetime for the Moderna booster is our model choice. Values for Infectiousness are adapted from Eyre et al. (2022), assuming a Moderna booster resembles the first two doses, and assuming Sinovac resembles ChAdOx1.

Parameter	Sinovac	Moderna booster	Label
Acquisition	0.5	0.93	η_A
Symptomatic given infection	0.08	0.26	η_S
Infectiousness	0.24	0.5	η_T
Hospitalisation given symptomatic	0.64	0	η_H
Death given hospitalisation	0.22	0	η_D
Expected lifetime	150	365	η_W
Expected time to seroconversion	14	14	η_C
Expected time before waning	28	60	η_M

between groups; ϵ is the reduction in infectiousness from asymptomatic relative to symptomatic individuals; p_3 and p_4 are the proportions of asymptomatic and symptomatic infectious days, respectively, spent self isolating, and $I_{\cdot,\cdot}$ is the vector of number of infectious asymptomatic ($I_{A,\cdot}$) and symptomatic ($I_{S,\cdot}$) people who are unvaccinated ($I_{\cdot,0}$), vaccinated ($I_{\cdot,1}$), or boosted ($I_{\cdot,2}$).

$$k_2 = (1 - p_S)/\sigma$$

is the rate to asymptomatic infectiousness, where $p_S = f_S(\eta_S, t)\widehat{p}_S$ is the probability to become symptomatic: a baseline probability $\widehat{p}_S$ modified by the vaccine effect $f_S(\eta_S, t)$, and σ is the expected duration of the latent period before the onset of infectiousness;

$$k_3 = 1/\gamma_A$$

is the rate of recovery from asymptomatic infection;

$$k_4 = p_S/\sigma;$$

is the rate of symptom onset;

$$k_5 = (1 - p_H)/\gamma_I$$

Table 10: Age-specific parameters from Knock et al. (2021)

Age group	Infection-hospitalisation rate	Infection-fatality rate
0 to 4	0.0300	0.0003
5 to 9	0.0026	0.0000
10 to 14	0.0008	0.0000
15 to 19	0.0004	0.0000
20 to 24	0.0008	0.0000
25 to 29	0.0026	0.0000
30 to 34	0.0040	0.0001
35 to 39	0.0063	0.0001
40 to 44	0.0120	0.0003
45 to 49	0.0190	0.0007
50 to 54	0.0230	0.0012
55 to 59	0.0400	0.0028
60 to 64	0.0960	0.0087
65 to 69	0.1000	0.0121
70 to 74	0.2400	0.0351
75 to 79	0.5000	0.0843
80 to 120	0.5000	0.0970

is the rate of recovery from symptomatic infection, where p_H is the probability to be hospitalised, and $\gamma_I = p_H \gamma_H + (1 - p_H)\gamma_R$ is the expected time to be in compartment I_S: γ_H is the expected duration before hospitalisation and γ_R is the expected duration before recovery.

$$p_H = (1 + p_\Delta h_\Delta) f_H(\eta_H, t)\widehat{p}_H$$

is the baseline probability to be hospitalised ($\widehat{p}_H$) adjusted by the vaccine effect protecting against hospitalisation ($f_H(\eta_H, t)$) and scaled up by the proportion of lineages that are type Delta, p_Δ, assuming that the Delta variant has hospitalisation rate h_Δ higher. Then

$$k_6 = p_H/\gamma_I$$

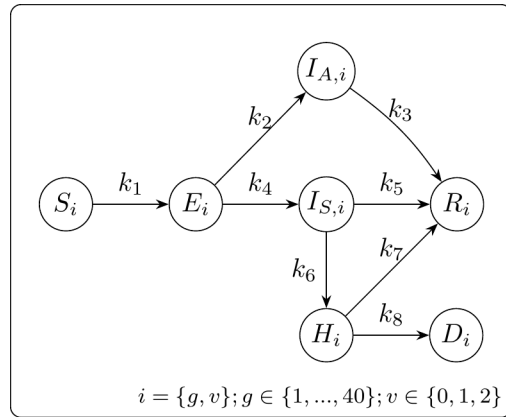is the rate of hospitalisation following symptomatic infection.

Figure 8: Disease state transitions

$$k_7 = (1 - p_D)/\lambda_H$$

is the rate of recovery of hospitalised patients, where p_D is the probability to die given hospitalisation, and $\lambda_H = p_D\lambda_D + (1 - p_D)\lambda_R$ is the expected time to be in compartment H: λ_D is the expected duration before death and λ_R is the expected duration before recovery (Djaafara et al., 2021).

$$p_D = f_D(\eta_D, t)\hat{p}_D$$

is the baseline probability to die ($\hat{p}_D$), adjusted by the vaccine effect protecting against death ($f_D(\eta_D, t)$). Finally,

$$k_8 = (1 + p_\Delta\mu_\Delta)(1 + \theta(H(t - 21)))p_D/\lambda_H$$

is the rate of death following hospitalisation, which is the initial rate p_D/λ_H, which corresponds to the rate of recovery, scaled up by the proportion of lineages that are type Delta, p_Δ, assuming that the Delta variant has fatality rate μ_Δ higher, and scaled further by a function θ of total hospital occupancy 21 days prior.

Note that, as we do not know from whom the sequenced viruses were taken and subsequently assigned lineages (whether infectious or hospitalised), we use the same fraction p_Δ for time t for all rates that are affected: rate of infection, rate of hospitalisation, and rate of death.

Changing the "rate of death" here without changing the "rate of recovery" changes the actual probability of death together with the expected duration in hospital. We explore the relationship between relative rate, probability and duration in Figure 9. This we present for context but note that the values are neither computed nor used. The adjustment to the rate would also be consistent with hospital duration shortening among those who die and staying the same among those who survive, for example. The only consequence of importance for understanding the model is that, given our mechanism for adjusting the rate of death, the expected duration of stay in hospital decreases when the rate of death increases.
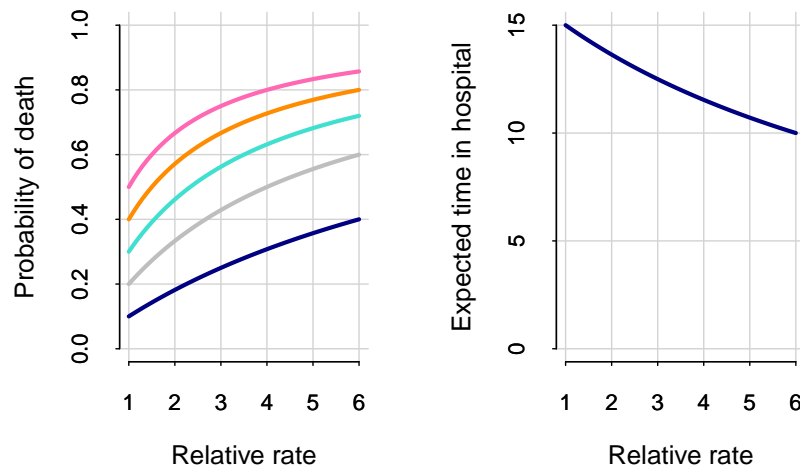
Figure 9: Probability of death as a function of rate of death, where the initial probability is 0.1,…,0.5. We compute the actual probability to die as $k_8/(k_7 + k_8)$, which depends on p_D and the amount by which the rate k_8 is increased from its baseline, $(1 + p_\Delta \mu_\Delta) \cdot (1 + \theta(H(t - 21)))$ (the "relative rate"). We can compute the corresponding expected time to be in hospital if we assume the durations are the same for those who recover and those who die.

B.1.1   Vaccination state transitions

Recently, booster shots have been administered in Indonesia to health workers. The vaccine used is Moderna, administered to health care workers who have had two Sinovac doses already. In our model, $v = 0$ refers to unvaccinated people, $v = 1$ to people who have received two doses of Sinovac, and $v = 2$ to people who have received two doses of Sinovac and a Moderna booster. How we model transitions between vaccination states and from recovery to susceptible is shown in Figure 10.

k_9 and k_{15} represent the rates of vaccination of unvaccinated susceptible and recovered people, and k_{16} and k_{17} represent the rates of boosting of vaccinated susceptible and recovered people. k_{13}, k_{14} and k_{18} represent the rates of recovered people returning to susceptibility. k_{10} is the rate of seroconversion to vaccine-induced immunity, and $k_{12}(t) = k_1(0, t)$ is the rate of infection of just-vaccinated people, which returns them to the unvaccinated epidemiological pathway.

B.2   Contact rates

As in the Daedalus model of Haw et al. (2020), the economic configuration is manifest in the epidemiological model via changes of compartment membership, and scaling of contact rates. In the original presentation of the model, the set $\{x_{i,\tau}\}$ (i.e. the sector opening) is used as the model input, and the set $\{w_{i,\tau}\}$ (i.e. the workforce present assuming a nonlinear production function) is used a replacement model input for a sensitivity analysis. Here, we use both sets as inputs to the epidemiological model, where $w_{i,\tau}$ determines movement of workers and contacts to workers. Meanwhile, $x_{i,\tau}$ scales contacts between consumers and workers, and $x_{i,\tau}^2$ scales contacts between school students, and between consumers in commercial settings.
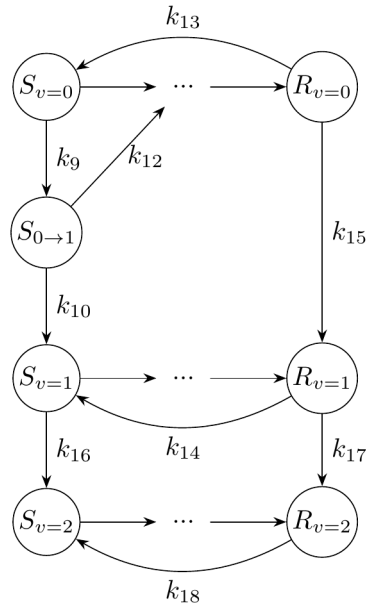
Figure 10: Vaccination state transitions

B.3 Vaccine waning

We model vaccine effect waning for people in compartment $S_{g,v}$, i.e. susceptible people in group g who have received two doses of Sinovac or a booster, so $v = 1, 2$. To capture the effect of waning for each population, we model the time-dependent amount of remaining vaccine effect among the group, V, which scales the effect of the vaccine. For simplicity, for the remainder of this section we omit the index g from $S_{g,v}$, and what follows applies to each group independently. We illustrate for vaccine $v = 1$ but the same is applied to $v = 2$.

B.3.1 Population average vaccine effect

Suppose each individual j has a remaining relative vaccine effect $0 \leq \phi_{j,t} \leq 1$ at time t. $\phi_{j,t}$ begins at 1 after a person is vaccinated and wanes to 0 over time. The total effect for the group at time t is

$$V(t) = \sum_{j=1}^{S_{v=1}} \phi_{j,t}.$$

B.3.2 Dynamics of the population average vaccine effect

The dynamics of $V(t)$ are determined by the vaccination schedule, vaccine waning, the booster schedule, infection events, and waning of natural immunity that returns recovered people to susceptibility. To allow for a period of maximum immunity before waning occurs, we split $V(t)$ into two parts: $V(t) = V_1(t) + V_2(t)$. $V_1(t)$ matures to $V_2(t)$ and does not wane; $V_2(t)$ wanes at a constant rate, corresponding to exponential decay.

All transitions determining the vaccine amount are shown in Figure 11. k_{21} is the rate of maturation from full vaccine effect to waning vaccine effect. $k_{11} = 1/\eta_W$ is the rate of waning of the effect once it starts to wane. The susceptible population is similarly split into $S_{v=1} = S_{v=1}^{(1)} + S_{v=1}^{(2)}$. Their rates of infection are k_{19} and k_{20}.
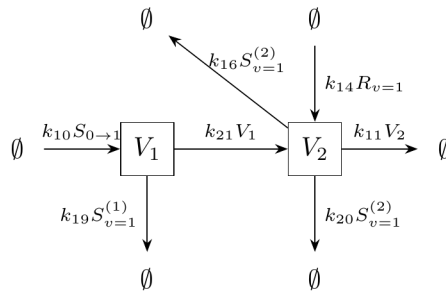
Figure 11: Dynamics of waning shown for vaccinations corresponding to $v = 1$. There is an analogous set of dynamics for $v = 2$, but without transitions corresponding to k_{14} and k_{16}.

B.3.3 Rates of infection

As $S_{v=1}^{(1)}$ people have full vaccine effect, $S_{v=1}^{(1)} = V_1$, and $S_{v=1}^{(2)} = S_{v=1} - S_{v=1}^{(1)}$ people have average relative vaccine effect

$$\hat{\phi}_t = \frac{V_2(t)}{S_{v=1}^{(2)}}.$$

$\hat{\phi}_t$ is the average residual vaccine effect for the group at time t, and scales the vaccine effect down from its maximum value (its effect in a group in whom no waning has occurred).

The value $\hat{\phi}_t$ determines the rate of infection. Recall from Equation (12) that the rate of acquisition of infection depends on the vaccine status v and the protective vaccine effect against acquisition η_A via function f_A. We define

$$f_A(v, \eta_A, t) = \begin{cases} 1 & v = 0 \\ 1 - q_1 \eta_{A,v} - q_2 \hat{\phi}_t \eta_{A,v} & v > 0 \end{cases}$$

where $\eta_{A,1}$ and $\eta_{A,2}$ are the maximum protective vaccine effects against acquisition for the initial double dose and the booster shot, respectively. The value for status v is the weighted sum of people with relative vaccine effect 1 and with relative vaccine effect $\hat{\phi}_t$. For the whole $S_{v=1}$ group, there are $S_{v=1}^{(1)}$ with full effect and $S_{v=1}^{(2)}$ with average effect $\hat{\phi}_t$, so $q_n = S_{v=1}^{(n)}/S_{v=1}$ for $n = 1, 2$.

B.3.4 Who gets infected

For the part of group $S_{v=1}$ with full vaccine effect ($S_{v=1}^{(1)}$), with reference to Figure 11, we have $k_{19} = (1 - \eta_{A,1})k_0(t)$, so that the flux out of V_1 is equal to the flux out of $S_{v=1}^{(1)}$: for every person who is infected, one quantity of vaccine effect is lost from the pool.

The flux out of V_2 represents how much of the $S_{v=1}^{(2)}$ group's vaccine effect leaves with each infection. We should expect this to be less than the average effect per person, as people with more waned immunity are more likely to be infected. We write it as

$$k_{20} = F_{I,t} \hat{\phi}_t (1 - \hat{\phi}_t \eta_{A,1}) k_0(t),$$

with $0 \leq F_{I,t} \leq 1$ representing the average vaccine effect among those who are infected at time t relative to the average in the group. We pre-calculate $F_{I,t}$ based on the vaccine rollout strategy, the time to develop immunity, the time to begin waning, and the rate of waning.

B.3.4.1 Distribution of ϕ over time For this derivation, we return to consideration of a population of people with unique vaccine effects $\phi_{j,t}$ for individuals j and days t. We describe the distribution of values over the population at time t as $p_\phi(\phi, t)$.

The time of maturation to waning effect for each person, t_M, uniquely defines their remaining vaccine effect at time t: $\phi = \exp\left(-(t - t_M)k_{11}\right)$. Then the probability to have value ϕ on day t is the probability to have matured on day t_M:

$$p_\phi(\phi, t) = p_M(t_M) = p_M(t + \log(\phi)/k_{11}).$$

The probability to have matured on day t_M is the probability to have been vaccinated on day t_V and to have taken $t_M - t_V$ days to seroconvert and mature. The former is given by $p_V(t_V)$, which is the probability that a person was vaccinated on day t_V (i.e. $t - t_V$ days ago), and is defined by the vaccination rollout schedule. The latter is described by a two-parameter hypoexponential distribution:

$$p_{MC}(t) = \frac{k_{21}k_{10}}{k_{21} - k_{10}}\left(\exp\left(-k_{10}t\right) - \exp\left(-k_{21}t\right)\right).$$

Then

$$p_M(t_M) \propto \sum_{t_V=0}^{t_M} p_V(t_V|t_V < t_M)p_{MC}(t_M - t_V).$$

B.3.4.2 Distribution of ϕ given infection From our estimate of the distribution of relative vaccine effect among the waning, susceptible population, we want to extract the distribution of those who would likely be infected.

Suppose there is one infection among $S_{v=1}^{(2)}$ at time t, and let η_A be the initial vaccine effect for protection against infection. The probability the person who was infected has relative vaccine effect ϕ is

$$p_I(\phi, t) = \frac{p_\phi(\phi, t)(1 - \phi\eta_A)}{\int_0^1 p_\phi(\phi, t)(1 - \phi\eta_A)d\phi}. \tag{13}$$

Then $f_I(\phi, t)$ is the expectation of $p_I(\phi, t)$ over ϕ:

$$f_I(\phi, t) = \int_0^1 p_I(\phi, t)\phi d\phi \tag{14}$$

This corresponds to the amount that each vaccinated person with waning immunity "carries out" when they leave the susceptible, vaccinated compartment.

B.3.4.3 Implementation We compute $f_I(\phi, t)$ with consideration of a number of transitions affecting the waning vaccine effect, but without consideration of infection events, the return of recovered vaccinated people to susceptibility, administration of booster doses, and delivery of second-dose vaccine to recovered rather than susceptible people. This will lead to a discrepancy between the expectation, $\hat{\phi}(t)$, given the distribution over ϕ we pre-compute, and the "true" distribution in the dynamic model that underlies the model average, $\hat{\phi}_t$. For this reason we use a fixed input

$$F_{I,t} = \frac{f_I(\phi, t)}{\hat{\phi}(t)}$$

which scales the model average value $\hat{\phi}_t$ to give us the expected average effect among those who are infected.

B.3.5 Summary of rate equations

In summary, the rate equations for $S_{v=1}$, V_1 and V_2 are:

$$\frac{dS_{v=1}}{dt} = k_{10}S_{0\rightarrow1} - k_1(1,t)S_{v=1} + k_{14}R_{v=1} - k_{16}S_{v=1},$$

$$\frac{dV_1}{dt} = k_{10}S_{0\rightarrow1} - k_{21}V_1 - k_{19}S_{v=1}^{(1)},$$

$$\frac{dV_2}{dt} = k_{21}V_1 - k_{11}V_2 - k_{20}S_{v=1}^{(2)} + \hat{\phi}k_{14}R_{v=1} - \hat{\phi}k_{16}V_2.$$

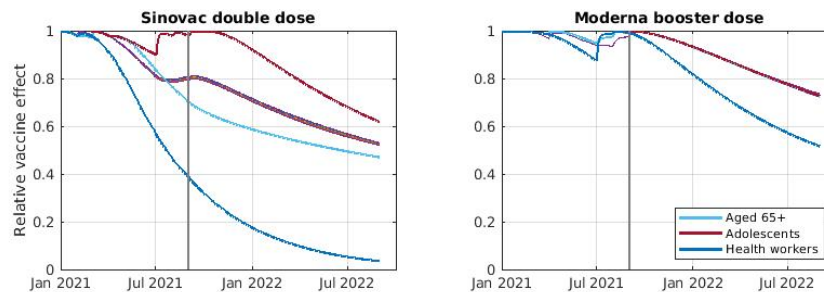The resulting average relative effect for each demographic group is shown in Figure 12.

Figure 12: The residual vaccine effect over time for the Sinovac double dose and the Moderna booster for all demographic groups, with adolescents, health workers and those aged over 64 shown in bold. The vertical lines indicate the beginning of the projection period, where both vaccines are rolled out. The projections correspond to Scenario 3, where 80% booster coverage is achieved in all three groups by the end of the period.

B.3.6 Other vaccine effects

For the other vaccine effects, including reduced infectiousness, reduced probability to be symptomatic, reduced probability to require hospitalisation given symptoms, and reduced probability to die given requiring hospitalisation, we use the waned vaccine effect from 21 days prior. This relies on two approximations: (1) that the past effect reflects the population-average vaccine effect when the pathway was entered, and (2) the average vaccine effect remains unchanged as individuals progress through the disease pathway. For example, defining $F(t) = F_1(t) + F_2(t)$, and $F_1(t) = k_{19}S_{v=1}^{(1)}(t)$ and $F_2(t) = k_{20}S_{v=1}^{(2)}(t)$ as the fluxes out of the $S_{v=1}$ compartment at time t, we can write the vaccine effect on the probability to be symptomatic at time t as depending on the mix of vaccine states among those who became infected t_S days earlier:

$$F_{S,t} = \frac{F_1(t - t_S)}{F(t - t_S)} + \frac{F_2(t - t_S)}{F(t - t_S)}\hat{\phi}_{t-t_S},$$

and $f_S(\eta_S, t) = 1 - F_{S,t}\eta_S$.

B.4 Hospital case fatality rate

Hospital case-fatality rate lags behind hospital occupancy by several weeks. This is likely due to hospital occupancy at time of admission being a more important determinant of outcome than hospital occupancy at time of death (or time of reporting of death).
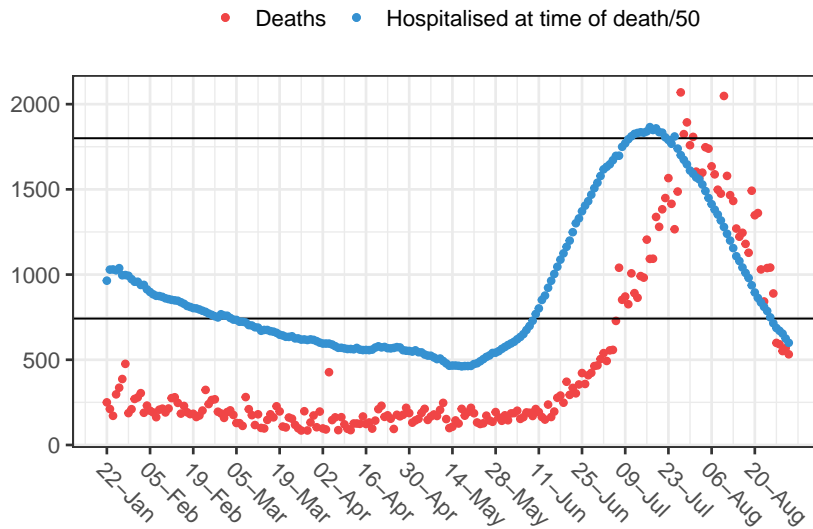
Figure 13: Hospital occupancy and deaths over time. Horizontal lines indicate H_{min} and H_{max}.

We model deaths as depending on hospital occupancy. Deaths occur at a constant rate for hospital occupancy < H_{min}, where H_{min}=37,100. Where occupancy exceeds H_{min}, the rate of death increases linearly. The amount the rate increases from hospital occupancy of H_{min} to H_{max}, denoted θ_0 and referred to as the HCFR surge rate, is learnt from the data:

$$\theta(H(t-21)) = \begin{cases} 1 & \sum H(t-21) < H_{min} \\ 1 + \theta_0 \frac{\sum H(t-21) - H_{min}}{H_{max} - H_{min}} & \sum H(t-21) > H_{min} \end{cases}$$

We fit the model to these data using a delay of 21 days for the surge rate. To account for the increased CFR for the Delta variant, we fit a parameter to allow an increase to the fatality rate of hospitalised patients over the period of its growth.

C   Fitting to data

Hospital occupancy data and death data (https://vaksin.kemkes.go.id/#/scprovinsi) are used to fit model parameters R_0, seed time, the hospital case fatality rate as hospital occupancy exceeds capacity (Table 11), and a 13-component time-varying modifier to transmission rate (Figure 14), which reflects changes in behaviour (or other factors) that affect transmission and are not captured by other model inputs (such as vaccinations and sector closures). All epidemic simulations use Matlab's delay differential equation solver dde23, and the parameters are fit using the optimisation function lsqcurvefit. Resulting fits are shown in Figure 15.
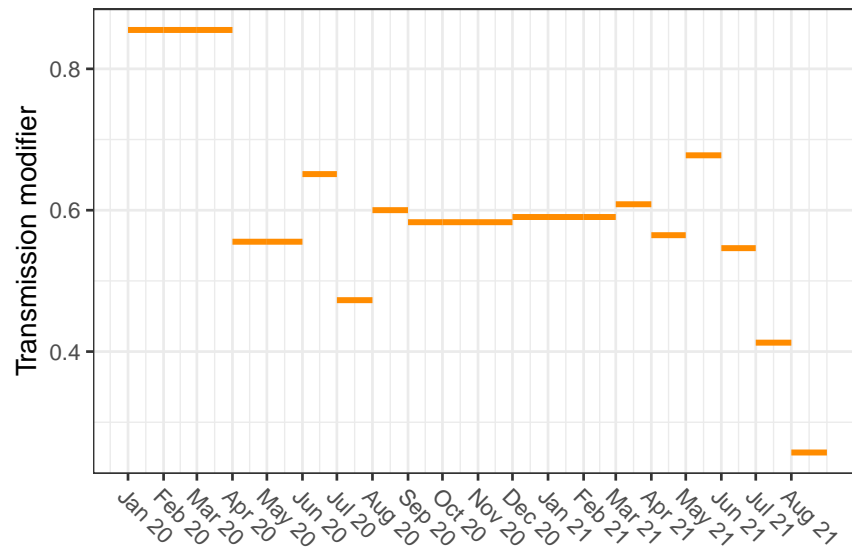
Figure 14: Modifier component of model that captures changing in transmission not attributable to business or school closures.
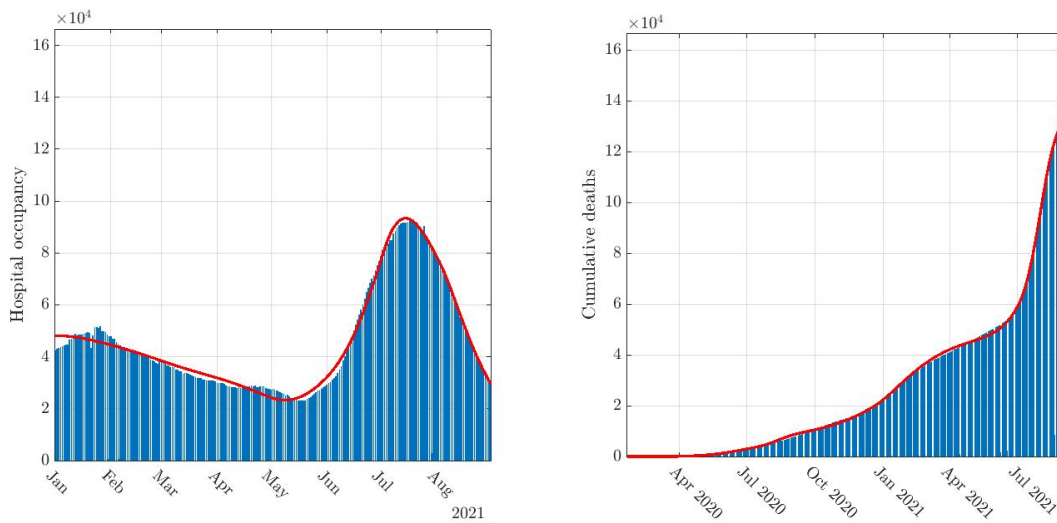

Figure 15: Data (blue) and model fit (red) for hospitalisations (left) and cumulative deaths (right) over time.

Table 11: Parameters fit to data. Inferred values for H_{min} and Hospital surge HFR imply that when hospital capacity goes from 37,100 to 90,000, the hospital case fatality rate increases by a factor of 3.3.

Parameter	Value
seed	-65.0
R_0	2.9
Hospital surge HFR	3.3
Delta HFR	0.7
H_{min}	37,100
Delta HR	1.9

D   Supplementary results

D.1   *Optimising for a short time horizon*

The Daedalus model is appropriate for short-term forecasting only, due to the uncertainty in how transmission will evolve. Policy decisions should be reviewed as data accumulate. However, optimising over a short time period leads to solutions that are sub-optimal in the longer term. In Figure 16 we explore the relationship between duration and solution.

The optimal short-term decision (i.e. the one that minimises the expected socio-economic costs under uncertainty for 2 months) is to have schools open 90% and sectors with a relative closure of 0.5. Given this configuration, the expected values for the number of deaths and the maximum hospital occupancy at the end of the period are high. Because the time horizon is short, much of the cost of the configuration choice is not realised until after the two months have passed. Indeed, the shorter the time period, the higher the hospital occupancy at the end of the period (up to a point). It is therefore worth considering longer time horizons, even if the objective is only to choose a configuration for two months.
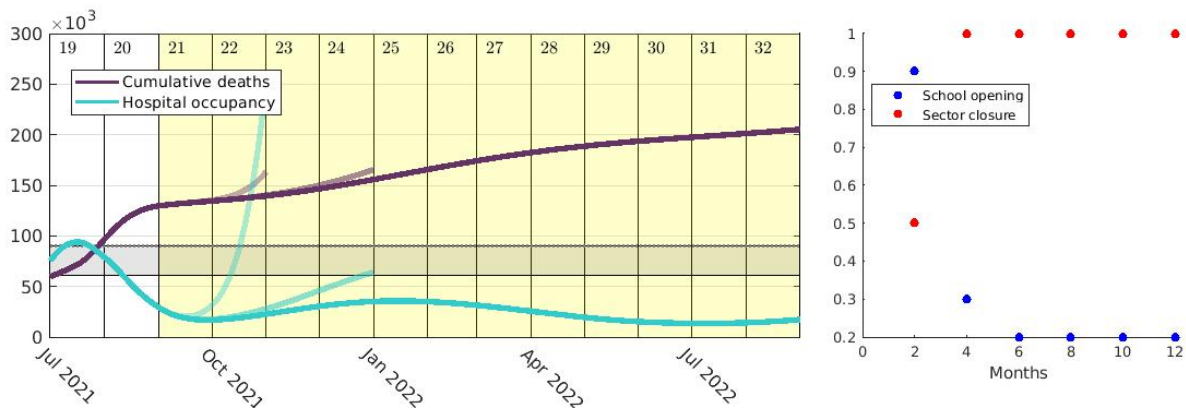

Figure 16: The optimal solution found depends on the duration of the period under consideration. Here we show optimal configurations (right) and epidemic trends (left) when the decision horizon is 2, 4, 6, ..., 12 months long. We choose from a decision space consisting of any combination of ten levels of school opening and nine levels of economic closure, where a relative closure of 1 corresponds to the configuration observed in April 2021, and we use Valuation 2 from Table 2 to define the socio-economic costs. We assume that Sinovac rollout continues for all people age five and older, and that there are no booster doses. The transmission modifier is constant and set to 0.55.

D.2   Booster rollout with different valuations

Table 12: Optimal pandemic mitigation configuration for three vaccine booster rollout scenarios, assuming alternative valuations for a year of life and a year of education.

Scenario	One-year target coverage, %	Doses (millions)	First four months		At ten months	
			School opening, %	Sector closure	School opening, %	Sector closure
VSY: $15,000. VLY: $42,000						
Scenario 1	0	0	40	3	60	3.3
Scenario 2	40	93.5	50	2.5	80	0.75
Scenario 3	80	187	50	2	100	0
VSY: $34,000. VLY: $42,000						
Scenario 1	0	0	50	3.5	70	3.85
Scenario 2	40	93.5	60	3.25	100	2.275
Scenario 3	80	187	60	2.5	100	0
VSY: $34,000. VLY: $80,000						
Scenario 1	0	0	50	3.75	60	3.75
Scenario 2	40	93.5	50	3	90	1.8
Scenario 3	80	187	60	3.25	100	0

The One-year target coverage is the percentage of adolescents, adults, and those over 65 given a booster dose by the end of the twelve-month period, and Doses is the total number of Moderna doses administered. These define the scenarios. School opening and sector closure are constant for the first four months, change linearly for the next six months, and are constant again for the final three months. Configurations are chosen to minimise socio-economic costs given the valuations under uncertain epidemic transmission.

Table 13: Benefit per dose for different valuations and vaccine coverages.

Value of school year ($)	Value of life year ($)	Benefit per dose ($)	
		40% coverage	80% coverage
15,000	42,000	2,200 (1,200-3,300)	2,000 (1,400-3,100)
15,000	80,000	2,500 (1,700-3,400)	2,000 (1,400-3,400)
34,000	42,000	3,600 (2,400-5,400)	3,000 (2,300-4,500)
34,000	80,000	4,200 (3,400-6,600)	3,300 (2,600-5,200)

Table 14: Socio-economic costs under three vaccine booster rollout scenarios, one year projection horizon, assuming alternative valuations for a year of life and a year of education

Scenario	Person-years of in-school education, millions[a]	Cost of education loss, billion $[b]	GDP, billion $[a]	GDP loss, billion $[b]	YLLs, millions[a]	Cost of YLL, billion $[b]	Deaths, millions[a]	Socio-economic costs, billion $	Saving, billion $
VSY: $15,000. VLY: $42,000									
Scenario 1	33	338	715 (714-715)	262 (262-265)	4 (0.16-20)	106 (4.22-515)	0.15 (0.006-0.72)	706 (604-1,120)	
Scenario 2	42	241	769 (768-770)	146 (145-147)	4.4 (0.18-19)	115 (4.81-491)	0.17 (0.007-0.68)	502 (391-880)	204 (110-310)
Scenario 3	50	166	796 (795-796)	91 (89.9-92.3)	3.2 (0.17-15)	84 (4.5-387)	0.12 (0.006-0.54)	341 (261-646)	365 (270-580)
VSY: $15,000. VLY: $80,000									
Scenario 1	30	369	707 (707-708)	286 (285-288)	2.2 (0.14-13)	113 (7.03-650)	0.086 (0.005-0.48)	768 (661-1,310)	
Scenario 2	39	277	769 (769-770)	145 (145-147)	2.2 (0.15-12)	111 (7.43-587)	0.085 (0.006-0.44)	533 (430-1,010)	235 (160-320)
Scenario 3	49	180	788 (787-788)	112 (111-113)	1.9 (0.14-9.9)	94.5 (7.19-497)	0.072 (0.005-0.37)	387 (299-791)	381 (260-640)
VSY: $34,000. VLY: $42,000									
Scenario 1	39	616	695 (694-696)	314 (312-316)	7.1 (0.18-27)	185 (4.78-698)	0.26 (0.007-0.95)	1,115 (933-1,630)	
Scenario 2	52	327	727 (727-728)	240 (238-242)	8.2 (0.25-25)	212 (6.53-642)	0.3 (0.01-0.88)	779 (572-1,210)	336 (230-510)
Scenario 3	54	277	782 (781-783)	122 (121-123)	5.8 (0.22-20)	150 (5.86-529)	0.21 (0.009-0.73)	549 (403-929)	566 (420-850)
VSY: $34,000. VLY: $80,000									
Scenario 1	36	685	692 (691-692)	324 (324-327)	4.5 (0.16-20)	224 (8.23-1,000)	0.17 (0.006-0.73)	1,233 (1,020-2,010)	
Scenario 2	45	478	741 (740-741)	208 (207-210)	3.2 (0.16-14)	159 (8.1-710)	0.12 (0.006-0.53)	845 (693-1,400)	388 (320-610)
Scenario 3	53	298	767 (766-767)	160 (159-162)	3.4 (0.18-14)	167 (8.97-695)	0.13 (0.007-0.51)	625 (466-1,150)	608 (490-970)

Expected values with 95% confidence interval in parentheses.

[a] Outputs from the epidemiological model (YLLs, Deaths) and economic model (Person-years of in-school education, GDP) for the configuration

[b] Costed losses compared to the no-pandemic counterfactual, which contribute to the socio-economic costs as defined in Equation 2 using the valuation sets from Table 2

D.3   Relevance in current circumstances: Omicron

In order to contextualise these results in the current moment of the pandemic, which is dominated by the Omicron variant in early 2022, we estimate what the costs would have been had Omicron been the predominant variant throughout the projection horizon. We re-run the same simulations and identify optimal decisions anew, assuming that the relative vaccine effect in preventing infection for the booster is 0.76 and for Sinovac is 0 (Andrews et al., 2021), the relative hospitalisation rate is 0.3, the relative hospital-fatality rate is 0.67 (Ferguson, Ghani, Hinsley and Volz, 2021), and the relative vaccine effects protecting against hospitalisation and hospital fatality are 0.5 and 0.6, respectively (Ferguson, Ghani, Cori, Hogan, Hinsley and Volz, 2021).

For the three scenarios, we find expected costs that are similar relative to the costs calculated for the respective main scenarios that assume the rates of hospitalisation and death and vaccine effects do not change, as presented in Table 5. The expected socio-economic costs relative to those reported in Table 5 are 98%, 104%, and 98%, respectively, for the three scenarios. That is, there is no systematic difference in the absolute value of the expected costs, nor in the expected costs relative to each other across scenarios. Therefore we have no reason to expect costs estimated in 2022 to be systematically different from those already estimated for the circumstances and time horizon beginning in September 2021 as a result of changes in the predominant variant, given the profile of viral effects we assume for each case.

Optimal configurations in these hypothetical scenarios require less stringent closures of business and school initially, but slower gradual opening. This is due to the expected nature of the variant having less severe outcomes but also being less responsive to vaccines.

Based on these results, we tentatively suggest that if we were to re-compute costs for a time horizon starting in 2022, we would not expect costs (or savings) to be systematically different because of the Omicron variant. However, this assumes all else is equal. In practice, computed costs may differ for reasons other than the characteristics of the predominant variant, such as progress since made in vaccination coverage, medical treatment, and the number of infections incurred in the interim. We show in Section D.4 how uncertainty in the virus profile included in the computation of the cost allows us to assess which parameter uncertainties drive uncertainty in the outcomes or, put another way, how much the projected outcome depends on the parameter.

D.4   Sensitivity analysis: uncertain variant profiles

We present the results for our main scenarios (see Table 5) with fading vaccine effects and two additional parametric uncertainties: the reduced vaccine effect in preventing infection, and change to hospitalisation rate (Figure 17). The distributions represent our uncertainties about future changes to the profile of the circulating viral population in August 2021. Our uncertainty about the change in hospitalisation rate is large: it includes what we might have expected based on variants observed up to that point (which all showed increased severity), and also allows for the hospitalisation rate to go down, reflecting emergence of variants causing less severe disease.

We model fading vaccine protection against infection as a linear decrease over the twelve-month period for protective effects for both Sinovac and Moderna vaccines, averaging over possible temporal population dynamics (i.e., times at which mutations occur and time taken to dominate the population). The decrease has an uncertain slope, ending in a final percent-reduction in the vaccine effect distributed as Beta(8,4), so that the median effect after twelve months is 68% (95% CI 39–89%) of its initial effect, approximately corresponding to the percentage change in estimates

of vaccine effectiveness between November 2020 and November 2021. For example, the Moderna vaccine was estimated to have a reduction of around 80% in effectiveness against the Delta variant (Rosenberg et al., 2021). If there are two such complete population shifts of the circulating virus in a year with compounded decreases to vaccine effect, the result would be a decrease to 64% effectiveness (see also Figure 17 for a comparison to the Omicron variant).

At the same time, new variants can result in different hospitalisation rates. Here, we allow for the rate of hospitalisation to change in the same way as we do the vaccine effect. We allow for it to increase to up to around 2.5 times, and to decrease to around 0.4 times, with a final value described with a lognormal distribution with log mean -0.1 and log standard deviation 0.5.
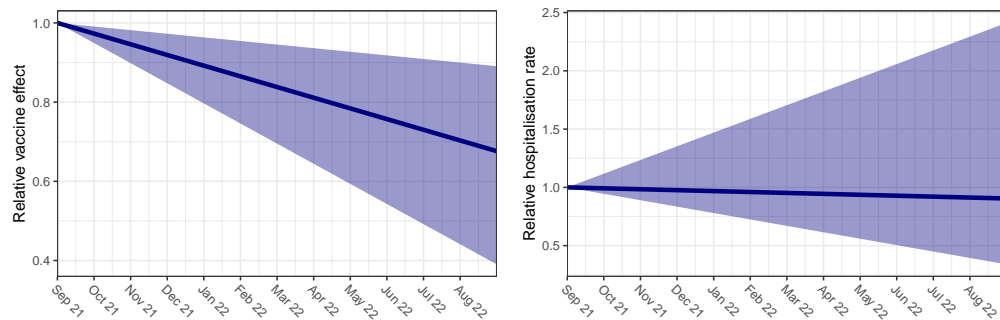

Figure 17: Our model of the effect of potential new variants on vaccine escape and hospitalisation rate. Values in the model are relative to the values at the beginning of the projection horizon.

We find that if vaccine effects fade over time and vaccine-effect fading and hospitalisation rates are uncertain, the expected benefit per vaccine dose is $2,400 for scenario 2 (95% CI 1,600–5,200) and $2,000 for scenario 3 (95% CI 1,500–3,900). Finally, we examine the relationships between the uncertain variables and the outcomes of interest (Figure 18). The total socio-economic cost and the saving in scenario 3 compared to scenario 1 are somewhat correlated with the uncertain transmission modifier, but not strongly with vaccine effect or hospitalisation rate, nor with a predictor that combines the two parameters.

The intuitions visualised in Figure 18 can be quantified with metrics such as value of information (Jackson et al., 2021), given in Table 16, which quantifies the impact of uncertainty in parameters on the uncertainty in the outcome. The higher the value, the more predictive the parameter is of the outcome. This type of analysis allows a policy maker to anticipate which uncertainties are most important to resolve in order to make a more accurate estimate of the cost, and therefore a more informed decision on whether booster vaccinations are a worthwhile investment. There is a limit to what we can learn about future transmission and future viral characteristics in order to make these predictions more accurate, but it is important to note how the conclusions we reach are variously sensitive or robust to these uncertainties. It provides some reassurance that the values estimated from the outlook of August 2021 are not very sensitive to the changing vaccine profile, consistent with the finding that the costs estimated assuming Omicron-like parameters were similar to those estimated previously. Instead, the costs are most sensitive to uncertain transmission. Modelling efforts to resolve these uncertainties would likely have most value in making cost estimations more precise.

Table 15: Socio-economic costs under three vaccine booster rollout scenarios, one year projection horizon, assuming an uncertain decline in vaccine effect and an uncertain change in hospitalisation rate over time.

Scenario	Person-years of in-school education, millions[a]	Cost of education loss, billion $[b]	GDP, billion $[a]	GDP loss, billion $[b]	YLLs, millions[a]	Cost of YLL, billion $[b]	Deaths, millions[a]	Socio-economic costs, billion $
Scenario 1	30	369	692 (691-692)	324 (324-326)	2.6 (0.14-17)	128 (6.91-861)	0.096 (0.005-0.63)	821 (699-1,560)
Scenario 2	36	308	749 (748-749)	189 (188-190)	2.1 (0.14-13)	103 (7.02-649)	0.079 (0.005-0.49)	600 (503-1,150)
Scenario 3	45	211	772 (772-772)	147 (146-148)	1.8 (0.14-12)	93 (6.93-605)	0.071 (0.005-0.45)	451 (364-963)

Expected values with 95% confidence intervals in parentheses.

[a] Outputs from the epidemiological model (YLLs, Deaths) and economic model (Person-years of in-school education, GDP) for the configuration

[b] Costed losses compared to the no-pandemic counterfactual, which contribute to the socio-economic costs as defined in Equation 2 using Valuation 2 from Table 2

Table 16: Value of information calculated using the R `voi` package (Jackson et al., 2021), reported as the percentage of variance of the outcome.

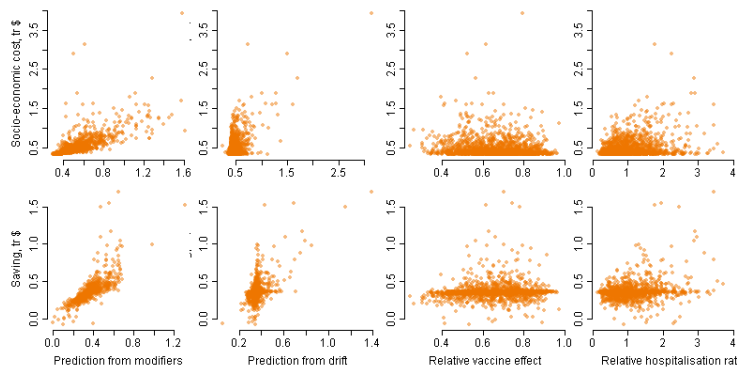| Outcome	Modifiers	Vaccine effect and hospitalisation rate	Vaccine effect	Hospitalisation rate
Socio-economic cost	64	15	1	10
Saving	51	8	1	5

Figure 18: How much do the uncertain variables determine our outcomes of interest? Outcomes of interest are the total socio-economic cost for Scenario 3, and the Saving made in Scenario 3 relative to Scenario 1. We summarise the uncertain variables as follows: The "Prediction from modifiers" is a summary of the transmission modifiers into a single variable that best predicts the outcome using the R package INLA. The "Prediction from drift" is a summary of the two drift parameters (vaccine effect and hospitalisation rate) estimated in the same way. The univariate relationships for those two parameters are shown in the final two columns.